Computing Hydraulic Conductivity from Borehole Infiltration Tests and Grain-Size Distribution in Advance Glacial Outwash Deposits, Puget Lowland, Washington

Bart Weitering

A report prepared in partial fulfillment of
the requirements for the degree of

Master of Science
Earth and Space Sciences: Applied Geosciences

University of Washington

October 2015

Project Mentors:
Curtis Koger, Associated Earth Sciences, Inc.
Jennifer Saltonstall, Associated Earth Sciences, Inc.
Lam Nguyen, Associated Earth Sciences Inc.

Internship Coordinator:
Kathy Troost

Reading Committee:
Michael Brown
Juliet Crider

MESSAGe Technical Report Number: 027

ABSTRACT

This study evaluates two methods for estimating a soil's hydraulic conductivity: in-situ infiltration tests and grain-size analyses. There are numerous formulas in the literature that relate hydraulic conductivity to various parameters of the infiltrating medium, but studies have shown that these formulas do not perform well when applied to depositional environments that differ from those used to derive the formulas. Thus, there exists a need to specialize infiltration tests and related grain-size analyses for the Vashon advance outwash in the Puget Lowland. I evaluated 134 infiltration tests and 119 soil samples to find a correlation between grain-size parameters and hydraulic conductivity. This work shows that a constant-head borehole infiltration test that accounts for capillarity with $\alpha \approx 5 m^{-1}$ is an effective method for calculating hydraulic conductivity from our flow tests. Then, by conducting grain-size analysis and applying a multiple linear regression, I show that the hydraulic conductivity can also be estimated by $\log(K) = 1.906 + 0.102D_{10} + 0.039D_{60} - 0.034D_{90} - 7.952F_{fines}$. This result predicts the infiltration rate with a 95% confidence interval of 20 ft/day. The study is funded by Associated Earth Sciences, Inc. (AESI), for application in the Puget Lowland.

TABLE OF CONTENTS

List of Figures **page**

List of Tables **page**

List of Appendices **page**

Key to Symbols

K = hydraulic conductivity

Q = flow rate

r = borehole radius

h = height of water in borehole; hydraulic head

L_A = length of borehole exposed to aquifer; screened interval

U = thickness of unsaturated zone above the water table

T_u = distance from water table to water level in borehole

C = conductivity coefficient

α = capillarity parameter

Ψ = pressure head

K_r = relative hydraulic conductivity

K_s = saturated hydraulic conductivity

K_h = saturated hydraulic conductivity in the horizontal directions, generally parallel to bedding

K_v = saturated hydraulic conductivity in the vertical direction, generally perpendicular to bedding

D_x = representative grain-size diameter which x% of the sample is finer than

F_{fines} = fraction of the soil by weight that passes the #200 sieve

$K_{infiltration}$ = hydraulic conductivity from borehole infiltration test

$K_{texture}$ = hydraulic conductivity from grain-size analysis

1 INTRODUCTION

1.1 Motivation

Hydraulic conductivity (K), the property of a material that describes the rate at which a fluid moves through it, is a parameter of fundamental importance in the geosciences. It has applications that range from agriculture to solute transport to oil reservoir characterization (Shepherd, 1989). One can measure hydraulic conductivity directly in the field or in the lab, but such tests are generally expensive and time-consuming. This paper will examine an alternative approach to measuring K.

One hydrologic application of interest in the Pacific Northwest is the design of stormwater infiltration facilities. Infiltration facilities reduce the hydrologic impacts of infrastructure development that increases the area of impermeable surfaces (Massmann, 2003). Impermeable surfaces decrease aquifer recharge and increase surface runoff, which can lead to problems like increased flooding, erosion, and pollution in waterways. Massmann's infiltration pond research for the Washington Department of Transportation yielded a potentially useful method to estimate hydraulic conductivity from grain-size parameters. Associated Earth Sciences, Inc. (AESI) sought to apply Massmann's result, but noticed that it consistently overestimated their field-measured hydraulic conductivities by up to two orders of magnitude (Nguyen, 2013).

Nguyen pursued a more appropriate result by using local field-measured hydraulic conductivity and by considering the difference between normally consolidated and over-consolidated sediments. He calculated field-measured hydraulic conductivities from pilot infiltration tests (PITs), which are designed to have a low head and large flat pit bottom infiltration area. Consequently, these tests yield an approximation of the vertical hydraulic conductivity, K_v.

Building on the work of Nguyen, AESI contracted this author (Weitering) to achieve an analogous result for high-head infiltration facilities like Underground Injection Control (UIC) wells. The infiltration area in UIC wells is primarily along the well screen or borehole wall, so it is suspected that the hydraulic conductivity from borehole infiltration tests is representative of K_h: the horizontal hydraulic conductivity. In a homogenous, isotropic soil, $K_h = K_v$. In the real world, however, K_h/K_v varies significantly with a typical value for layered deposits being 10 (Curtis Koger, personal communication, 2014). Thus, there exists a need to be able to determine K_h independently of K_v.

1.2 Scope of Work

The purpose of this study is to evaluate the relationship between field-measured hydraulic conductivity and grain-size distribution for high-head borehole infiltration tests. The objectives are (1) to identify a formula that effectively computes the hydraulic conductivity for borehole infiltration tests, (2) to calculate representative grain-size parameters from sieve data, and (3) to perform a multiple linear regression between field-measured K and grain-size parameters. The form of the resulting linear regression is motivated by the designs of Massmann (2003) and Nguyen (2013).

1.3 Geologic Setting

The Puget Lowland lies between the Canadian border to the north, the Cascades to the East, and the Olympics to the west. Its southern boundary is defined by the extent of Pleistocene glaciation, which is approximately at the boundary between the Puget Sound and Chehalis River drainage basins near Tenino, Washington (Vaccaro et al., 1998). The broad topographic low reflects a structural low that is the forearc basin resulting from Cascadia subduction. The present day topography is a product of repeated glaciation and tectonic deformation, superimposed by alluvial processes, landslides, and human development (Troost and Booth, 2008). The result is a complex and incomplete succession of glacial and non-glacial deposits that can vary in texture significantly over short distances.

During the past 2.4 million years at least seven major glacial advances have scoured the landscape and deposited sequences of sediments characteristic of glacial environments. The most recent glacial maximum is the Vashon stade of the Fraser glaciation, which occurred roughly 15,000 years ago and deposited much of the present-day surface geology. As the Vashon glacier grew southward and entrained sediment, meltwater rivers emanating from the glacier deposited stratified sands called advance outwash. These deposits consist mostly uniform fine to medium sand but also contains random interbeds of gravel, gravelly sand, sandy gravels, silty sand, and silt. As it grew south the ice then overrode this advance outwash and deposited till, which is a heterogeneous mixture of clay, silt, sand, and gravel in an unsorted, unstratified layer deposited directly without being reworked by meltwater. As the glacier retreated, it again deposited outwash sand and, in some circumstances, glaciolacustrine or glaciomarine clays. Due to the enormous weight of the overriding ice sheet, advance outwash can be considerably denser than recessional outwash (Booth, 1994). All of the injection wells examined in this work are completed in advance outwash deposits.

2 BACKGROUND

2.1 In-Situ Testing

Perhaps the best known field method for estimating hydraulic conductivity is an aquifer (or "pumping") test. One conducts this test by stimulating an aquifer via pumping and then observing the resulting head change in one or more monitoring wells. Aquifer tests yield a representative value of K_h over a large volume. Though useful, aquifer tests are not always the preferred method for measuring K. If the extra time and expense of a large-scale test is not justified, one may acquire an estimate of the hydraulic conductivity through small-scale in-situ tests such as the Guelph Permeameter (Elrick and Reynolds, 1985), Auger Hole and Inverse Auger Hole methods (Oosterbaan and Nijland, 1994), and other infiltration tests. Alternatively, undisturbed cores or disturbed soils can be taken to a laboratory for further hydraulic analysis using permeameters. The problem with these tests is that small samples are not typically representative of the whole deposit.

Nguyen performed small-scale PITs that filled 12-32 ft^2 holes with water 6" deep. By maintaining this low hydraulic head, one can assume that the late-time hydraulic gradient beneath the surface is equal to unity. This Green-Ampt approximation then leads to a relatively simple calculation of K_v (Nguyen, 2013). The Auger Hole methods feature a geometry closer to that of the borehole infiltration test while maintaining the PIT's simplicity by again assuming that hydraulic gradients are equal to unity. If there is a large ponded head in the infiltration facility, however, this assumption breaks down and a more complex formalism is required (Zangar, 1953).

The United States Bureau of Reclamations (USBR) adopted the landmark solutions of Glover and Zangar (1953) for calculating hydraulic conductivity from constant head borehole infiltration tests. These formulas (Eq. 1, 2) are widely applied throughout the world in geologic and water management engineering (Reynolds, 2013). Q is the flow rate, r is the well radius, h is the hydraulic

$$K = Q/(rhC) \quad (1)$$

$$K = 2Q/[rC(T_u+h-L_A)] \quad (2)$$

head, and T_u is the distance between the regional water table and the water level in the well. L_A is the length of the screened or open interval that is beneath the water level in the well. The two formulas

apply to two different scenarios (Figure 1). In the first case, the water table is deep below the bottom of the borehole and has negligible influence on fluid flow. As the water table nears the borehole, though, ponding causes flow rate from the borehole to decrease and Eq. 2 must be applied. This is because the water table acts as a lower boundary to the flow system, causing water to spread more laterally and decreasing hydraulic gradients (Stephens, 1979). One must consult Figure 2 to determine whether the deep or shallow water table conditions apply. Glover's coefficient C (Eq. 3)

$$C = (2\pi h/r)/[\sinh^{-1}(h/r) - 1] \quad (3)$$

$$C = 2\pi(2L_A h - L_A^2)/\{rh[\sinh^{-1}(L_A/r) - L_A/h]\} \quad (4)$$

was amended by Zangar (1953) to account for partially cased boreholes (Eq. 4) in the deep water table scenario. The two formulas' derivations differ only in the limits of integration along the borehole (Stephens, 1983). These derivations rely on several common assumptions:

- the soil is homogeneous and isotropic
- the soil is not subject to shrinking or swelling
- the effects of air trapped in pores or dissolved in water are negligible
- the water injected does not react chemically with the medium
- the borehole is free from mud cake, silt, and algal growth
- the water envelope becomes a cylinder at depth
- the flow rate from the borehole increases linearly with depth
- the flow field is completely saturated

The final assumption implies that capillary forces are neglected. This would later be shown to be the weakest assumption of the first generation of borehole infiltration test formulas (Stephens, 1979). In the USSR, Nasberg and Terletskata independently accomplished a similar derivation under the assumption that flow rate from the borehole is constant with depth (1954). Stephens (1979) found that his numerical methods suggested the Nasberg-Terletskata formula might be more accurate than Glover's solution in practice, despite its differing assumption being physically less realistic. Reynolds, Elrick, and Topp (1983) reexamined the derivation of the Glover solution and derived a formula

from their own pressure source distribution. Cornwell (1951) and Winger (1960) made early contributions as well, but ultimately the Glover solutions won the most widespread acceptance.

The second major advance in borehole infiltration tests was the inclusion of capillarity beginning with the work of Stephens, who noted that the C(h,r) relationship was more complex than previously thought. "Part of the non-unique behavior in the C… relationship is due to well geometry, and part is due to unsaturated soil properties" (1979). Stephens found semi-empirical formulas for four type sediments that account for the influence of capillarity. For example, one of the four soils was a sand "similar to" sand 4107 in Mualem's catalog (1978) which was found to have a conductivity coefficient given by Equation 5. Stephens' hypothetical sand had $\alpha = 4.62\ m^{-1}$, while sand 4107 in Mualem's catalog (Table 1) has $\alpha = 6.0\ m^{-1}$. Stephens also published a formula (Eq. 6) that was generalized to all soil textures by introducing the capillarity parameter α.

$$\log(C) = -0.381\log(r) + 0.162h/r + 0.951 \quad (5)$$

$$\log(C) = -0.658\log(h/r) - 0.238\alpha^{1/2} - 0.398\log(h) + 1.343 \quad (6)$$

Capillarity (α) is characterized by the hydraulic conductivity – pressure head (K-Ψ) relationship that is unique for each soil. Stephens (1979, 1987) defines α as the slope of the $\ln(K_r)$ - Ψ curve over the range $1.0 < K_r < 0.5$. K_r, the relative hydraulic conductivity, is the ratio of hydraulic conductivity at a given pressure head K(Ψ) to the saturated hydraulic conductivity K_s (in this paper, denoted as K_h or K_v). It is worth noting that hysteresis is neglected; only the properties of wetting soils are used to measure α. The value of the capillarity parameter is approximately equal to the inverse of the length of the capillary fringe. In coarse soils with weak capillary effects, α tends to be large and vice versa. Typical values of α are between $1.0\ m^{-1}$ and $10.0\ m^{-1}$ (Laase, 1989). Mualem's Catalog (Table 1) and Reynold's guidelines (Table 2) provide a good reference for values of α over a range of soils. In neglecting capillarity, the original Glover solution essentially assumed $\alpha = \infty$. Elrick and Reynolds (1992) suggest that $12.0\ m^{-1}$ is a better uninformed assumption, and that just about any field evaluation of α is clearly better than setting it equal to ∞. They also note, "Setting $\alpha = \infty$ is equivalent to assuming zero capillarity because of extremely coarse soil texture or very highly structured soil. The K_∞ value is not the same as the K calculated by the Glover analysis although it also assumes zero capillarity. The Glover solution achieves zero capillarity by setting $\Psi = 0$ (i.e. saturated conditions), which is… physically different from assuming a steep K-Ψ curve".

Another interesting caveat is that, although one might anticipate a consistent relation between K and α (i.e. high K soils have a large α and low K soils have a small α), the data do not always bear this out (Elrick and Reynolds, 1989). A final note on capillarity is that, "For any particular soil it seems logical to expect that, as h decreases, the size of the saturated zone near the borehole also decreases; and because the unsaturated zone is closer to the borehole, capillarity exerts an increasing influence on flow rate" (Stephens, 1979). Conversely, as h increases, the saturated zone grows larger and the influence of capillarity on flow rate decreases. Thus, in cases where $h >> r$ or when the infiltrating medium is extremely coarse, capillarity may be safely ignored and the Glover solution is an acceptable approximation. However, in most cases it is preferable to estimate the capillarity.

Following Stephens' seminal work, several authors attempted to derive their own formulas to better encapsulate unsaturated soil properties in infiltration testing. Reynolds, Elrick, and Clothier (1985) introduced unsaturated effects into their derivation by utilizing the Richards equation instead of the Laplace equation. Philip (1985) followed the Glover methodology but assumed a different shape for the saturated bulb. Neither Philip nor Glover were correct about the shape of the saturated zone, however. It turns out that only a small portion of the flow field near the borehole is saturated, and the cross sectional area normal to the flow path continues increasing with depth below the borehole. Another shortcoming of Philip's solution is that he assumes the effects of gravity and capillarity can be decomposed, when in reality, they cannot (Laase, 1989). Stephens et al. (1987) published a second

$$\log(C) = 0.486\log(h/r) + 0.4\alpha^{-1} - 0.454\log(h) + .019(h/r)^{1/2} + 0.828 \quad (7)$$

solution in which they refined his formula for C(α) (Equation 7). That was Stephens' final academic work on the topic before entering the private sector. Reynolds et al. have continued publishing on the topic (e.g. Elrick, Reynolds, and Tan 1989; Reynolds, Elrick, and Clothier 1992; Reynolds 2010), but their methodology has remained largely unchanged. Most recently, Reynolds (2013) sought to reconcile the differences between his solutions based on the Richards equation and the USBR solutions based on the Laplace equation. He found that, "USBR estimates were accurate (<25% error) when $h/r > 10$, $\alpha > 12.0\ m^{-1}$, $h > 10$ cm, and $L_A/r > 10$, but could overestimate or underestimate by up to an order of magnitude when outside those figures." The solution considering capillary effects, on the other hand, was always deemed accurate.

2.2 Laboratory Testing

Grain-size analysis has been a tool for geologists since its proper inception by Krumbein (1934) and going back to Hazen (1892). It is useful, for example, in distinguishing between different depositional environments. Grain-size analysis yields information such as soil texture and the degree of sorting, which are related to the hydraulic conductivity. "Since hydraulic conductivity is the measure of the ease with which fluid flows through the porous medium, certain relationships are expected to exist between hydraulic conductivity and the statistical parameters that describe the grain-size distribution of the depositional medium" (Alyamani and Sen 1993). Hazen's well-known

$$K \propto D_{10}^2 \tag{8}$$

formula (Equation 8) was the first empirical formula which attempted to describe this relationship (1892). D_x denotes the grain diameter which x% of the sediment sample is finer than. In well-sorted sediments, permeability is proportional to the square of the grain diameter (Krumbein and Monk, 1943). Shepherd (1989) performed a survey of the literature and found that the constants in Hazen's formula actually varied for different depositional environments. The exponents ranged from 1.11 to 2.05, with an average of 1.72. The constant of proportionality was generally higher for more texturally mature samples. Alyamani and Sen used the difference between D_{50} and D_{10} to estimate K (1993). They argue that more weight should be given to the finer half of the grain-size curve because, "The addition of large diameter grain-sizes to fine sizes will not alter the hydraulic conductivity, but the contrary is not true. Adding fine sizes to large grain-sizes will have a very significant effect on the hydraulic conductivity." Rogiers et al. (2012) argued that nearly the entire particle-size distribution curve contains useful information. Nguyen attempted to incorporate the entire grain-size curve by performing a multiple linear regression with D_1, D_2, D_3, …D_{99}, D_{100}, but he found that large multiple linear regressions led to overdetermined systems and unstable solutions (Lam Nguyen, personal communication, 2014). While those solutions worked perfectly for the sampled data, they could yield unreasonable results when applied to new data. Thus, there exists a tradeoff in precision and accuracy between using too few or too many grain-size parameters to characterize hydraulic conductivity. Nguyen (2013) found an effective compromise in the methodology of Massmann (2003), which used the grain-size parameters D_{90}, D_{60}, D_{10}, and F_{fines} -- the fraction of the soil, by weight, which passes a #200 sieve. D_x is the parameter in millimeters.

(9) $\log(K) = -1.57 + 1.90D_{10} + .015D_{60} - .013D_{90} - 2.08F_{fines}$

(10) a. $\log(K) = 0.99 + 1.47D_{10} - .071D_{60} + .010D_{90} - 8.31F_{fines}$

b. $\log(K) = 0.88 + 1.01D_{10} - 7.59F_{fines}$

Massmann's (2003) formula (Equation 10) yields K in cm/s, and Nguyen's (2013) formula (Equation 9) gives K in in/hr. Massmann's and Nguyen's results are of particular interest because of their application in the Puget Lowland. Recall that Nguyen's (2013) formula is from over-consolidated outwash while Massmann didn't distinguish over-consolidated from normally consolidated deposits. According to Massmann, "The resulting regression equation is then assumed to be valid for other similar soils." This is important because there are numerous empirical formulas in the literature used to compute hydraulic conductivity from grain-size distribution. Shepherd (1989) and Rosas et al. (2014) recognized, too, that equations for one depositional environment may not work well for samples from another depositional environment. Therefore, regression formulas that will be applied in the Puget Lowland should be derived from data which are collected in the Puget Lowland.

3 METHODS

3.1 Borehole Infiltration Tests

Data analyzed in this project come from AESI's database of project information from the past decade. AESI conducts flow tests that are essentially borehole infiltration tests. In these tests, water is injected into a well via hose and the observed head rise is recorded by hand in ~5-minute intervals and by a datalogger in ~10-second intervals. The tests are usually conducted in multiple steps. For the first few hours, water flows into the well at a constant rate monitored by a flow meter and the head is allowed to equilibrate. The flow meter has a 1-4 % measurement uncertainty (Icenta, 2015). Upon measuring the head, the flow rate is turned up and the head response is once again observed and recorded. Some flow tests have up to five steps. Each test step then becomes one (Q,h) data point for a given medium and well geometry. Altogether, the data comprises 134 test steps from flow tests in 60 different wells on 9 different projects within the Puget Lowland (Figure 3).

Although the head rise is usually small by the end of a step, AESI's procedure is not a true *constant head* borehole infiltration test. The USBR (2001) considers the head rise to be sufficiently small

("constant") when it becomes less than 0.2 ft/5 min. This is only true for about half of AESI's step tests. To resolve the discrepancy, I chose to extrapolate the head vs. time plots using a French Curve (Figure 4) until $dh/dt = 0$. The French Curve has long been a favorite tool of hydrogeologists for extrapolating data (Mike Brown, personal communication, 2015). In practice, this maneuver only had a small effect on calculations of K. Since a larger head rise for a given infiltration test would result in a lower hydraulic conductivity calculation, the effect of extrapolating data with the French Curve is that this analysis should estimate conservative values of K.

Another wrinkle in the methodology involves well completions. AESI's flow tests use wells which typically have open boreholes, PVC machine slotted, or .010" wire-wrapped screens. Some wells have pea gravel or sand backfill and some wells have no backfill. The USBR solution originally included the term effective radius (r_e), which was equal to the product of the well radius and the percent open area of the well screen. Later works, however, have ignored the distinction between r_e and r. For the purpose of this research I do not differentiate between well designs, either.

Given these modifications, one can now address the first objective in the Scope of Work: to find a formula that effectively computes the hydraulic conductivity from AESI's flow tests. In order to do this, I collected all of the relevant data such as Q, r, h, L_A, and depth to the water table (U) for each step of each infiltration test and entered them into a spreadsheet (Appendix A). I then apply Eq. 4-7, testing a range of possible α. I've chosen to focus on the Laplace-based Glover and Stephens equations and not the Richards-based Reynolds equations because the Glover solution explicitly evaluates the shallow water table scenario and the Reynolds' formula does not. Finally, I compare the constant-head borehole infiltration test results with independent K measurements from AESI's pumping tests in order to determine which formula and which values of α are most appropriate for analyzing the advance outwash sand of the Puget Lowland.

3.2 Grain-Size Analysis

While drilling infiltration wells, AESI occasionally excavated soil samples and returned them to the geotechnical laboratory for further testing. The samples underwent mechanical grain-size analysis using a stack of sieves in accordance with ASTM: D422 *Standard Method for Particle-Size Analysis of Soils*. The initial results show what percentage of the sample, by weight, passes through a series of

increasingly fine sieves. The instrumental error for this measurement is ~1% (Nguyen 2013). I retrieved the data from AESI's database and applied the MS Excel algorithm D_x_solver (Nguyen 2013), a linear interpolation method, in order to calculate the grain-size parameters D_{90}, D_{60}, D_{10}, and F_{fines}. One could visually pick these parameters from a grain-size curve, but for the purpose of consistency it is preferable to automate the process. Altogether, this data comprises 119 soil samples from 33 well installations on 7 projects.

Given the hydraulic conductivity from flow tests and values for grain-size parameters from sieve tests, one can finally perform a multiple linear regression modeled after Massmann (2003) and Nguyen (2013). A new twist in the application to deep wells is that there can be numerous soil samples taken at different depths for a single well. Thus, care must be taken to ensure that the proper D_x are regressed against the correct hydraulic conductivity. It is critical to keep track of the screened interval; obviously, only soil samples from depths where the infiltrating water is present during a particular test should be used to analyze that test. When there are multiple soil samples that contribute to a single step of the flow test, the K's predicted from grain-size parameters are averaged using the harmonic mean. This is the most appropriate technique for averaging vertical data (Massmann, 2003). To calculate the mean K for an aquifer by averaging over space (i.e. several wells), the geometric mean is best (Fetter, 2001). My least-squares linear regression uses MS Excel's Solver tool to minimize the sum of the squares of the differences between the K from flow tests ($K_{infiltration}$) and the mean K from relevant grain-size analysis ($K_{texture}$). The Solver runs the Evolutionary engine to produce a best fit between $K_{infiltration}$ and $K_{texture}$ by varying the coefficients in Eq. 9-10. Once the numerical method finds the best solution, coefficients of the resulting regression equation are simply read from the Excel spreadsheet.

4 RESULTS

4.1 In-Situ Hydraulic Conductivity

The results of the borehole infiltration test analyses are shown in Figure 5 and Appendix B. As expected, the Stephens (1979) solutions (Eq. 5-7) predict a larger hydraulic conductivity than the

original Glover (1953) solution (Eq. 4). The Stephens equations with 1.0 $m^{-1} < \alpha < 10.0\ m^{-1}$, which includes the sand similar to sand 4107 ($\alpha \sim 4.6$), generally predicts a hydraulic conductivity 2 to 7 times of that predicted by the original Glover solution. Judging from Tables 1 and 2, $\alpha \approx 5.0\ m^{-1}$ seems reasonable. The influence of capillarity on the Stephens solutions is shown in Figure 6. It is interesting to note the difference in behavior between the 1979 and 1987 equations (Eq. 6-7). The first solution begins with a nonzero K at $\alpha = 0$ and becomes large at $\alpha \rightarrow \infty$ with a concave up curve. The second solution begins with K (0) = 0 and goes asymptotic at $\alpha \rightarrow \infty$, maintaining a concave-down curve. The two solutions intersect near α=1 and α=10, between which $K_{1987} > K_{1979}$ (Figure 7). It is tempting to pick α from one of these intersections, but neither value seems ideal for advance outwash sand. I've elected to use Equation 5 (i.e. $\alpha \sim 4.6$) to calculate $K_{infiltration}$ for the multiple linear regression, not only because it reflects a reasonable value of α, but also because it was one of the original index soils which Stephens studied in detail in order to derive Eq. 6-7 in the first place.

4.2 Linear Regression with Grain-Size Distribution

Appendix C shows the interpolated particle-size distributions for all soil samples. Site D appears to have the most fines, followed by Site C and Site E. Site A has a relatively even mixture of fine and coarse samples. Site B and Site G have coarser sediments and then the single Site F sample has the coarsest grain-size curve. These preliminary observations are consistent with Figure 5: that is, the coarser soils generally have a larger hydraulic conductivity than those containing more fines. The precise relationship between particle-size distribution and hydraulic conductivity is revealed in the multiple linear regression (Appendix D). For AESI's borehole infiltration tests, my result is that hydraulic conductivity is best predicted from particle-size distribution according to Equation 11.

$$(11) \qquad \log(K_{infiltration}) = 1.906 + 0.102D_{10} + 0.039D_{60} - 0.034D_{90} - 7.952F_{fines}$$

A plot of K predicted from grain-size by Equation 11 vs. K measured by infiltration tests using Equation 5 shows a moderate correlation with $R^2 = 0.65$ (Figure 8). The standard error is 10.6 ft/day, so the 2σ 95% confidence interval is roughly 20 ft/day.

5 DISCUSSION

5.1 Comparison with Pump Test results

One way to independently verify the results is by comparing them to other field tests of hydraulic conductivity. Pumping tests are more expensive and time-consuming than infiltration tests, so AESI only conducted pumping tests at a handful of locations. None of the wells used for infiltration tests were also used for pump tests, but some pump tests did take place in the vicinity of infiltration wells. At Site A, a pump test on MW-28 yielded K_h = 13 ft/day and for MW-29 estimates K_h = 20 ft/day. Pumping MW-1 on Site D revealed K_h = 23 ft/day. For MW-4 at Site H, K_h = 25 ft/day. Table 3 shows how these values compare to the infiltration tests. Advance outwash has a coarsening upward pattern (Curtis Koger, personal communication, 2014). The pumping wells are deeper than the injection wells, so pump tests sample a finer part of the aquifer and thus should yield lower values of K than the infiltration tests. These pumping test results are consistent with both the average $K_{infiltration}$ and $K_{texture}$ values for each site (Appendix B), supporting the preferred use of Eq. 5 and my assessment that the value of α in advance outwash sand of the Puget Lowland is likely around 5 m^{-1}.

5.2 Evaluation of Regression Formulae

Another fruitful exercise is to compare my result, Equation 11, with the grain-size regression equations from Massmann (2003) and Nguyen (2013). From Figure 9 it is clear that Massmann's equation (Eq. 9) over predicts and Nguyen's equations (Eq. 10) under predict K compared to the present solution. My result is closer to that of Nguyen, who found that Massmann's equations over predict K by up to two orders of magnitude. On average over the range 1 ft/day<K<100 ft/day, Nguyen's Equations 10a and 10b predict K that are 61% and 46% of that predicted by Equation 11, respectively. Nguyen's PITs measured K_v while the borehole infiltration tests were believed to measure K_h, so this observation is consistent with the principle that $K_h > K_v$.

But is the borehole infiltration test truly a good indicator of K_h? According to Stephens (1979), "One cannot conclude that constant head tests give a value of K which is closer to K_h, as suggested by Winger". "If the soil is anisotropic and K in the analytical formulae is interpreted to be the principal hydraulic conductivity in the horizontal direction, its value may be underestimated by

several hundred percent. If K is interpreted to be the value in the vertical direction, its value may be grossly overestimated" (Stephens and Neumann, 1982). While the present result may not give values of K which are closer to K_h than to K_v per se, the results from constant head borehole infiltration tests are clearly closer to K_h than the vertical results from PITs. If K_h or K_v are unknown, a general rule of thumb is that $K_h \sim 10K_v$. From Figure 9 we see that $K_{infiltration} \sim 2K_v$. Thus, it is reasonable to conclude that Stephens' evaluation is fair; $K_{infiltration}$ actually lies somewhere between K_h and K_v.

5.3 Uncertainties and Future Work

One significant unknown in the second generation of borehole infiltration tests is the capillarity parameter α. In this research I've selected a single representative value of α and applied it uniformly for all infiltration test analyses. Perhaps a better approach would be to assign specific values of α for each individual infiltration test. One could assign α's based on Mualem's Catalog (1978), but an even more robust method would be to measure α in the field. For example, one could measure soil water potentials using a tensiometer or psychrometer and measure moisture content with a neutron probe or by gravimetric sampling (Stephens, 1979). Using an appropriate soil moisture retention curve, one could then determine the K(Ψ) relationship and the α parameter. A significant drawback is that these field measurements of α are only feasible for the shallow subsurface. Alternatively, one might be able to estimate α by measuring the height of the capillary fringe. But even if one were to measure capillarity for the near surface only, it would still be interesting to characterize this variation of α throughout advance outwash sand of the Puget Lowland.

Other approaches include numerical modeling to calculate $K_{infiltration}$. Reynolds and Elrick (1985) recognized that, "Although a numerical solution will, in general, be more accurate for a specific set of conditions, an analytical solution is more generally applicable and reveals the major physical relationships inherent in C". In addition to that reason, I adopted analytical solutions because AESI requested a simple algorithm that could easily be applied in the field. Theoretically, a numerical solution should provide more realistic $K_{infiltration}$, which in turn should lead to a better regression for $K_{texture}$. On the other hand, one could also try improving $K_{texture}$ by using different soil texture parameters such as Krumbein and Monk (1943) who used mean particle size and *standard deviation* to characterize K. Their statistical analyses assumed a log-normal particle-size distribution; adapting the methodology to account for skewness and kurtosis could make for an interesting study.

Modelling would be particularly useful to further examine the Site D dataset, as it contains extremely detailed grain-size information (sampled every 2.5' from the surface to 80'). Additional flow tests with multiple steps could make Site D a very interesting case study. Furthermore, numerical modelling could also be used to evaluate the applicability of these analytical solutions to deep wells with large hydraulic heads. According to Stephens et al. (1987), "the borehole permeameter is an in-situ technique to test a relatively large sample size *at any depth*". However, his semi-empirical formulas for C only involve data from depths down to only 15m. The Guelph permeameter is only designed for infiltration test depths of only a couple of meters, but Reynolds (2013) too suggests his solutions are applicable at greater depths. Whether or not this is really true remains uncertain.

Other questionable assumptions include the soil being homogenous and isotropic, a handful of soil samples being representative of the entire aquifers, and the type of well completion being insignificant. We've treated borings with soil samples from multiple depths as if the geology is layered, with each layer having the texture of the soil sample taken at that depth. Ultimately the numbers are averaged and each well test step is matched to one representative $K_{texture}$, but by treating the site as a layered system we've technically violated the common assumption that the subsurface is homogenous and isotropic. Furthermore, the samples which define each "layer" may not even be representative of the actual soil at that depth. Glacial deposits can be irregular, varying in texture significantly over short distances. One should be more skeptical of borings where only one or two soil samples exist (e.g. Site B, Site C, and Site F). It is possible that the samples are from lenses of relatively coarse or fine material that don't represent the larger infiltrating volume. In Nguyen's PITs (2013), pits were over-excavated following the infiltration test in order to document the soils that water infiltrates into. In the borings for these high-head infiltration tests, however, there are no samples from beneath the wells (where much of the infiltrating volume is located). While those common assumptions may be problematic, they are unavoidable. But unlike homogeneity and representativeness, one should be able to quantify the impact of well completions. I do not know why the literature dropped the term r_e for r, but using r instead of r_e did produce much more sensible results. We hypothesized that this could be because the well screen manufacturers are conservative in their listed transmitting capacity. The head rise during infiltration tests should be due to the formation's transmissivity: not that of the well screen. Nonetheless, I find it plausible that the type of well completion does influence the infiltration rate.

6 CONCLUSIONS

Two common methods for estimating a soil's hydraulic conductivity are infiltration tests and grain-size analyses. A shortcoming of these methods is that certain coefficients are not constant from one depositional environment to another. This work adapts the constant-head borehole infiltration test for AESI's flow tests in advance outwash sand of the Puget Lowland. After calculating $K_{infiltration}$, the result from each flow test step entered into a multiple linear regression with particle-size parameters derived from mechanical grain-size analyses of the infiltrating media. The results show that a second generation constant-head borehole infiltration test that accounts for capillarity, such as those of Stephens (1979, 1987), works best with $\alpha \approx 5\ m^{-1}$. Assuming sand 4107 is representative of advance outwash sand, the linear regression with particle-size parameters yields the empirical formula $\log(K) = 1.906 + 0.102D_{10} + 0.039D_{60} - 0.034D_{90} - 7.952F_{fines}$. The hydraulic conductivity predicted by this new formula is approximately twice that predicted by Nguyen (2013). Since Nguyen's method predicts K_v, and K_h/K_v is usually ~10, I infer that the hydraulic conductivity from borehole infiltration tests is neither purely K_h nor K_v. Suggestions for future work include field measurements of the capillarity parameter α, scrutinizing the influence of different well completions, and numerical modeling to study the effects of scaling on borehole infiltration tests.

7 REFERENCES

Alyamani, M.S., and Sen, Z. "Determination of Hydraulic Conductivity from Complete Grain-Size Distribution Curves." *Ground Water* 31 (1993): 551-555.

ASTM Standard D422, 2007, "Standard Test Method for Particle Analysis of Soils," ASTM International, West Conshohocken, PA, 2007, DOI: 10.1520/D0422-63R07E02, www.astm.org.

Booth, Derek. "Glaciofluvial Infilling and Scour of the Puget Lowland, Washington, during Ice-sheet Glaciation." GSA Special Publications 22.8 (1994): 695-98.

Daube, Klaus. "Drawing and Illustrating in the Pre-digital Time." Drawing Tools. 2001. Web. 15 Dec. 2015. <http://www.daube.ch/docu/glossary/drawingtools.html#french_curves>.

Elrick, D.E., and W.D. Reynolds. "Methods for Analyzing Constant Head Well Permeameter." *Soil Science Society of America* 56.1 (1992): 320-23.

Elrick, D.E., W.D. Reynolds, and K.A. Tan. "Hydraulic Conductivity Measurements in the Unsaturated Zone Using Improved Well Analyses." *Groundwater Monitoring & Remediation* 9.3 (1989): 184-93.

Fetter, C.W. "Properties of Aquifers." Applied Hydrogeology. 4th ed. Upper Saddle River: Prentice-Hall, 2001. 88.

Hazen, A. "Experiments upon the purification of sewage and water at the Lawrence Experiment Station." *Massachusetts State Board of Health 23rd Annual Report.* 1892.

"Flow Meter Selection Guide: Choosing the Right Flow Meters." Flow Meter Selection Guide. Icenta, 2015. Web. 15 Dec. 2015. <http://www.icenta.co.uk/selectionguide/Flow>.

Krumbein, W.C. "Size Frequency Distributions of Sediments." *Journal of Sedimentary Petrology* 4.2 (1934): 65-77.

Krumbein, W.C., and G.D. Monk. "Permeability as a Function of the Size Parameters of Unconsolidated Sand." *Transactions of the American Institute of Mining and Metallurgical Engineers* 151 (1943): 153-63.

Laase, Alan D. A Critical Evaluation of Borehole Permeameter Solutions. MS thesis. New Mexico Institute of Mining and Technology, 1989.

Massmann, Joel. Washington State. Department of Transportation. *A Design Manual for Sizing Infiltration Ponds.* 2003. <http://www.wsdot.wa.gov/research/reports/fullreports/578.2.pdf>.

Massmann, Joel. Washington State. Department of Transportation. *AN APPROACH FOR ESTIMATING INFILTRATION RATES FOR STORMWATER INFILTRATION DRY WELLS*. 2004. <http://www.wsdot.wa.gov/research/reports/fullreports/589.1.pdf>.

Massmann, Joel. Washington State. Department of Transportation. *Implementation of Infiltration Ponds Research*. 2003. <http://www.wsdot.wa.gov/research/reports/fullreports/578.1.pdf>.

Mualem, Yechezkel. "Hydraulic Conductivity of Unsaturated Porous Media: Generalized Macroscopic Approach." *Water Resources Research* 14.2 (1978): 325-34.

Nguyen, Lam. *Evaluation of the Relationship Between Saturated Hydraulic Conductivity and Grain-Size Distribution of Fluvio-Glacial Deposits, Puget Lowland, Washington*. MS thesis. University of Washington, 2013.

Olanrewaju, J., and Wong, T. "Hydraulic Conductivity, Porosity, and Particle-size Distribution of Core Samples of Upper Glacial Aquifer: Laboratory Observations." Department of Earth and Space Sciences, State University of New York, Stony Brook, NY. 2010. <https://dspace.sunyconnect.suny.edu/bitstream/handle/1951/48010/ORLANRE00.pdf?sequence=1>.

Oosterban, RJ and Nijland, HJ (1994). Determining the saturated hydraulic conductivity. In: Ritzema HP (ed.) Drainage Principles and Applications (2nd edn.). ILRI Publication 16, Netherlands. 435-476.

Philip, J.R. "Approximate Analysis of Borehole Permeameter in Unsaturated Soil." *Water Resources Research* 21.7 (1985): 1025-033.

Reynolds, W.D. "An Assessment of Borehole Infiltration Analyses for Measuring Field-Saturated Hydraulic Conductivity in the Vadose Zone." Engineering Geology 159 (2013): 119-30.

Reynolds, W.D. "Measuring Soil Hydraulic Properties Using a Cased Borehole Permeameter." Vadose Zone Journal 9 (2010): 637-52.

Reynolds, W.D., and Elrick, D.E., and G.C. Topp. "A Reexamination of the Constant Head Well Permeameter Method for Measuring Saturated Hydraulic Conductivity Above the Water Table." *Soil Science* 136.4 (1983): 250-68.

Reynolds, W.D., D.E. Elrick, and B.E. Clothier. "The Constant Head Well Permeameter: Effect of Unsaturated Flow." *Soil Science* 139.2 (1985): 172-80.

Rogiers, B., D. Mallants, O. Batelaan, M. Gedeon, M. Huysmans, and A. Dasargues. "Estimation of Hydraulic Conductivity and Its Uncertainty from Grain-Size Data Using GLUE and Artificial Neural Networks." Math Geoscience 44 (2012): 739-63.

Stephens, Daniel. "Analysis of Constant Head Borehole Infiltration Tests in the Vadose Zone." diss., New Mexico Institute of Mining and Technology, 1979. <http://arizona.openrepository.com/arizona/bitstream/10150/191055/1/azu_td_hy_e9791_1979_451_sip1_w.pdf>.

Stephens, Daniel "In Situ Determination of Hydraulic Conductivity in the Vadose Zone Using Borehole Infiltration Tests." Technical Completion Report, New Mexico Institute of Mining and Technology, 1983. < http://wrri.nmsu.edu/publish/techrpt/tr180/tr180.pdf>.

Stephens, D.B., and S.P. Neumann. "Free Surface and Saturated-Unsaturated Analyses of Borehole Infiltration Tests Above the Water Table." Advanced Water Resources 5 (1982): 111-16.

Stephens, Daniel B., Kevin Lambert, and David Watson. "Regression Models for Hydraulic Conductivity and Field Test of the Borehole Permeameter." Water Resources Research 23.12 (1987): 2207-214.

Terletskata, N.M. "Determination of Permeability in Dry Soils." *Hydroelectric Waterworks* 2 (1954).

Troost, K.G., and D.B. Booth. "Geology of Seattle and the Seattle Area, Washington." Landslides and Engineering Geology of the Seattle, Washington Area 20 (2008): 1-35.

United States. Department of the Interior, Bureau of Reclamation. *Earth Manual*. Denver, CO, 1998. <http://www.usbr.gov/pmts/materials_lab/pubs/earth.pdf>.

United States. Department of the Interior, Bureau of Reclamation. *Engineering Geology Field Manual*. Denver, CO, 2001. <http://www.usbr.gov/pmts/geology/geolman2/Chapter17.pdf>.

Vacarro, J., Hansen, A., & Jones, M. (1998). Hydrogeological Framework of the Puget Sound Aquifer System, Washington and British Columbia. USGS Professional Paper, 1424-D.

Xiang, Jiannan. "Improvements in Evaluating Constant-Head Permeameter Test Data." *Journal of Hydrology* 162 (1994): 77-97.

Zangar, Carl. United States. Department of the Interior, Bureau of Reclamation (USBR). *Theory and Problems of Water Percolation*. Denver, CO: 1953. <http://www.usbr.gov/pmts/hydraulics_lab/pubs/EM/EM08.pdf>.

FIGURES

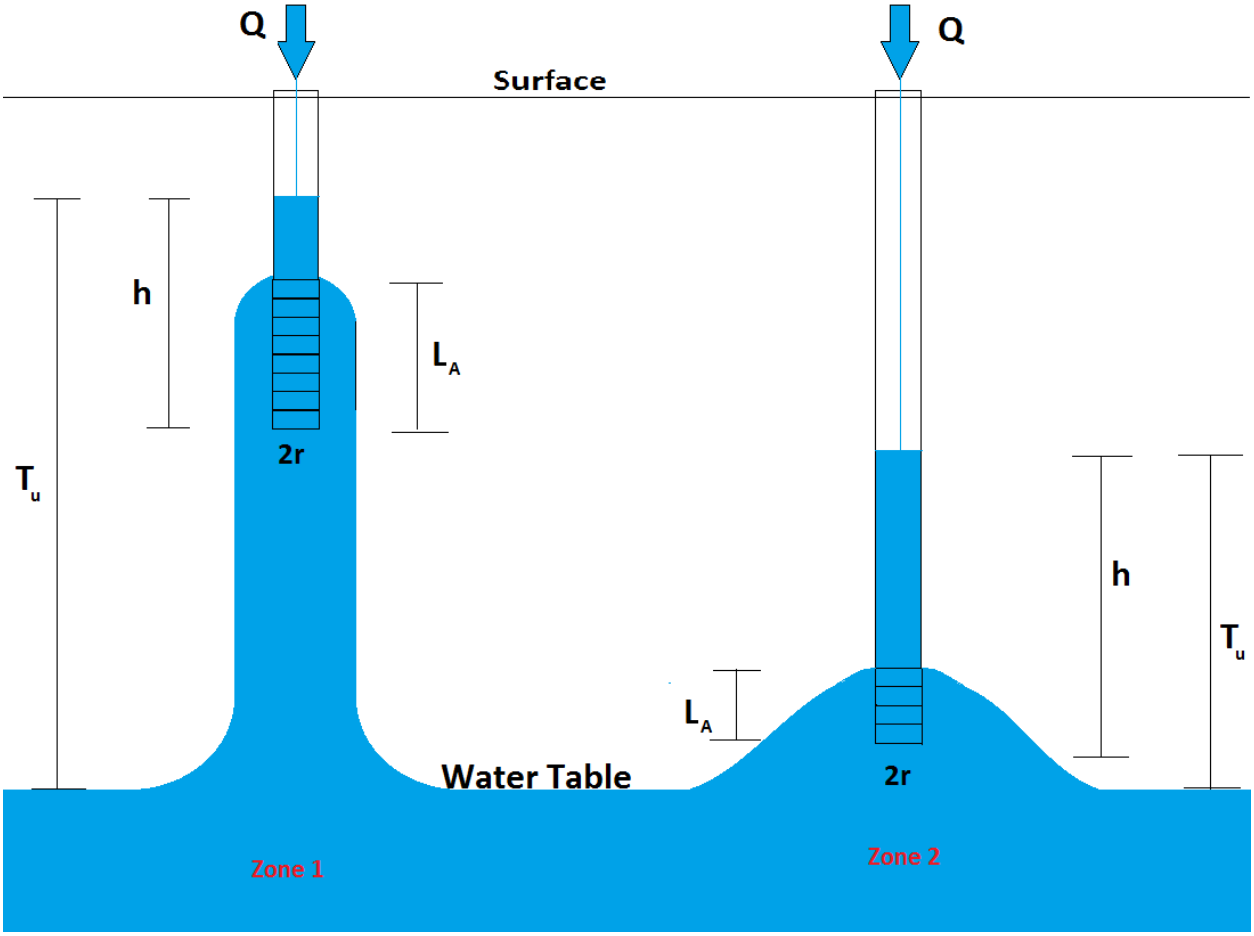

Figure 1. Experimental setup showing the relevant variables and the conceptual difference between the shallow water table and deep water table scenarios

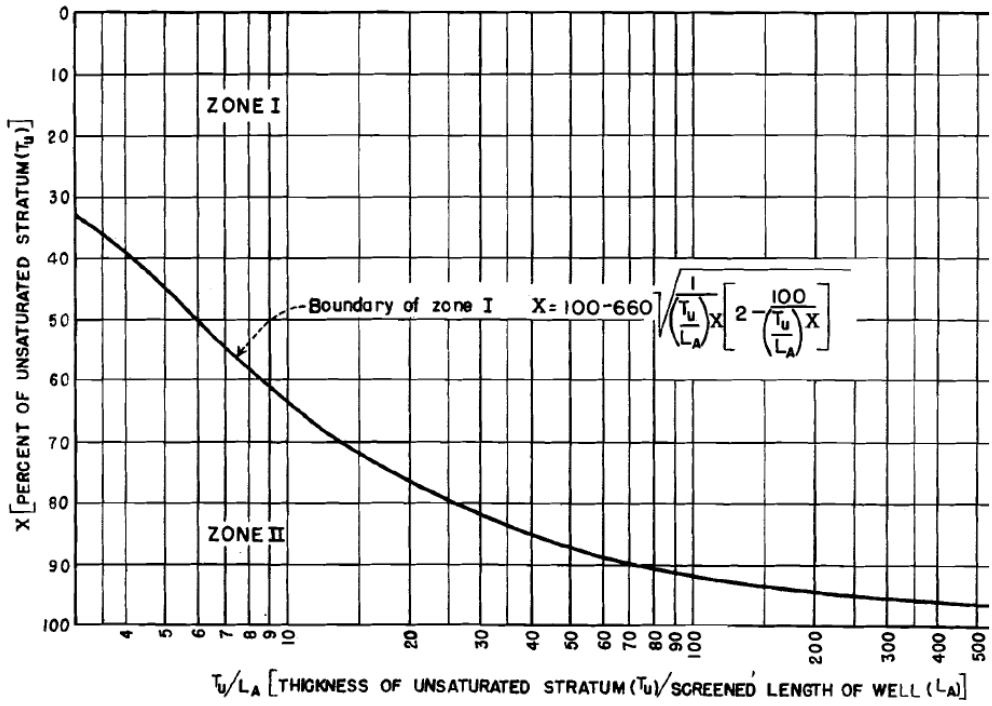

Figure 2. Chart used to determine whether to select the deep (zone I) or shallow (zone II) water table formalism (Zangar, 1953)

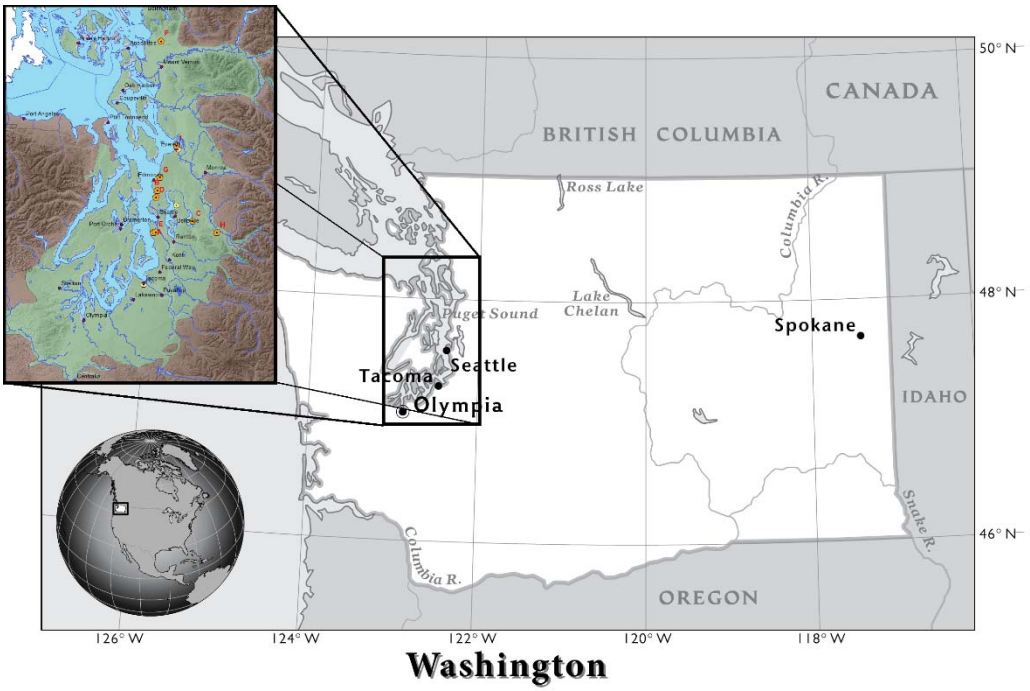

Figure 3. (a) Regional Setting

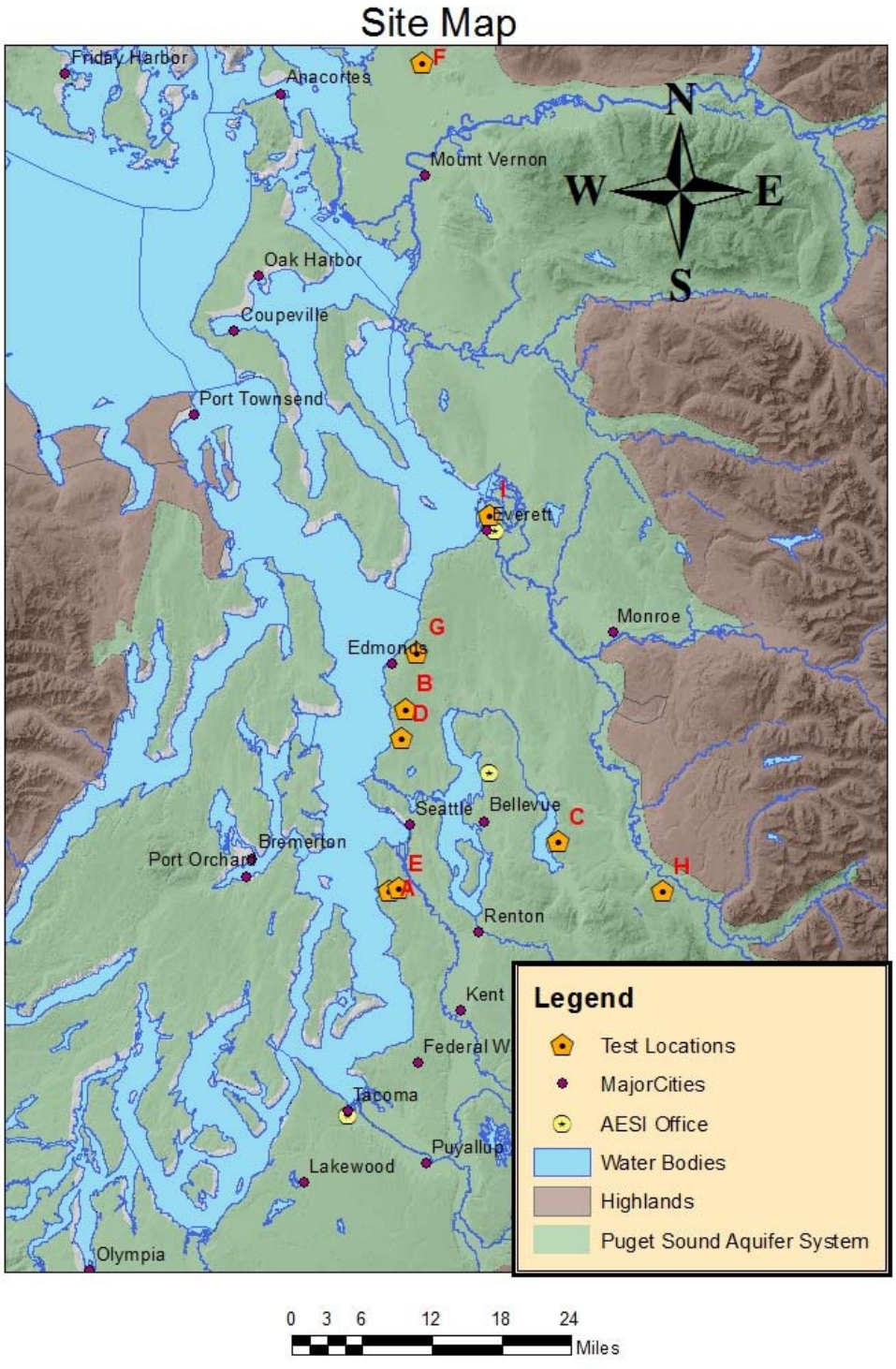

Figure 3. (b) Local Setting

Figure 4. "A common set of [French] curves is the Burmester set displayed here. The first item is very handy for ellipses, the second very often fits large parts of hyperbolas and the third (largest) item is used most for parabolas" (Daube, 2001)

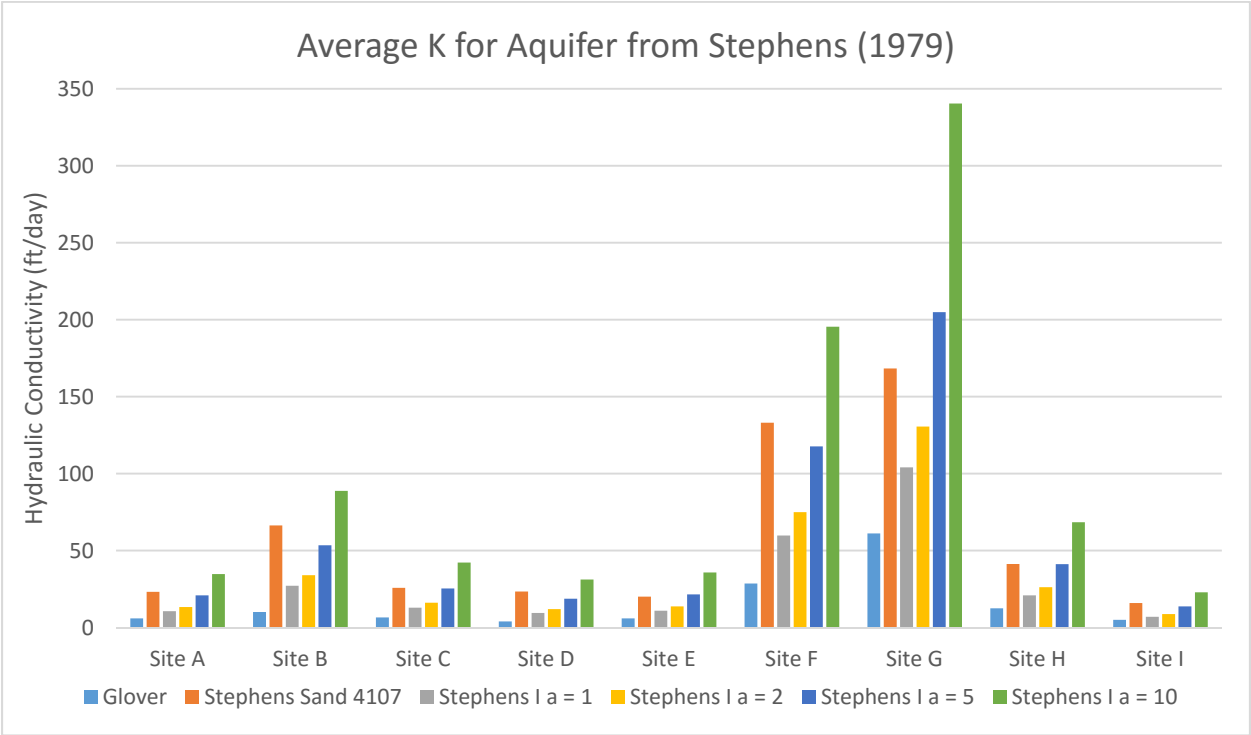

Figure 5. (a) Results using borehole infiltration tests (Stephens, 1979) for different α

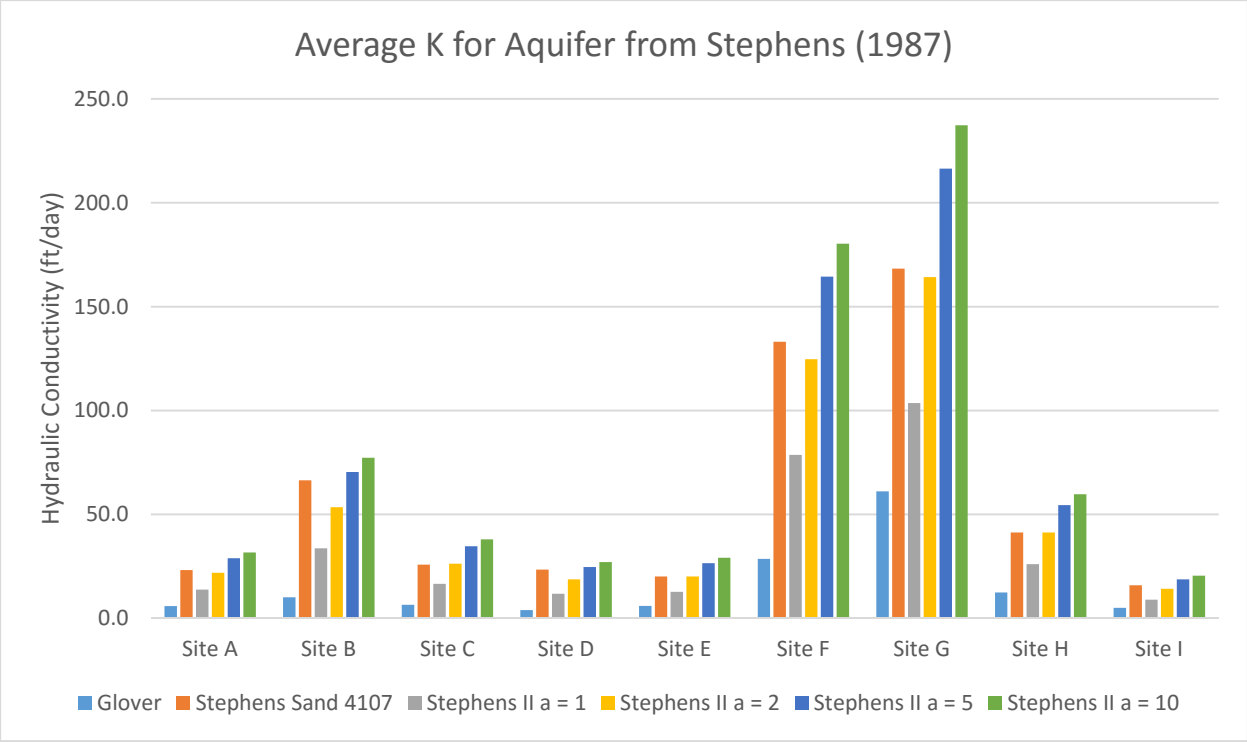

Figure 5. (b) Results using borehole infiltration tests (Stephens et al., 1987) for different α

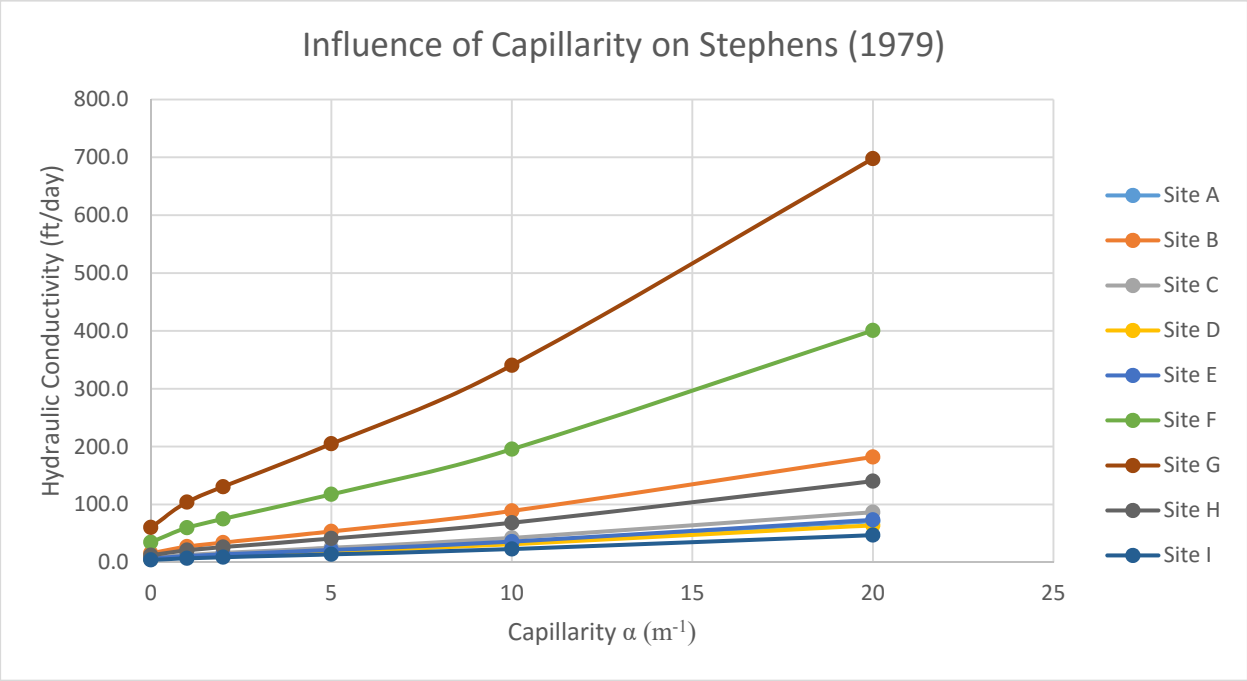

Figure 6. (a) K(α) for the Stephens (1979) solution

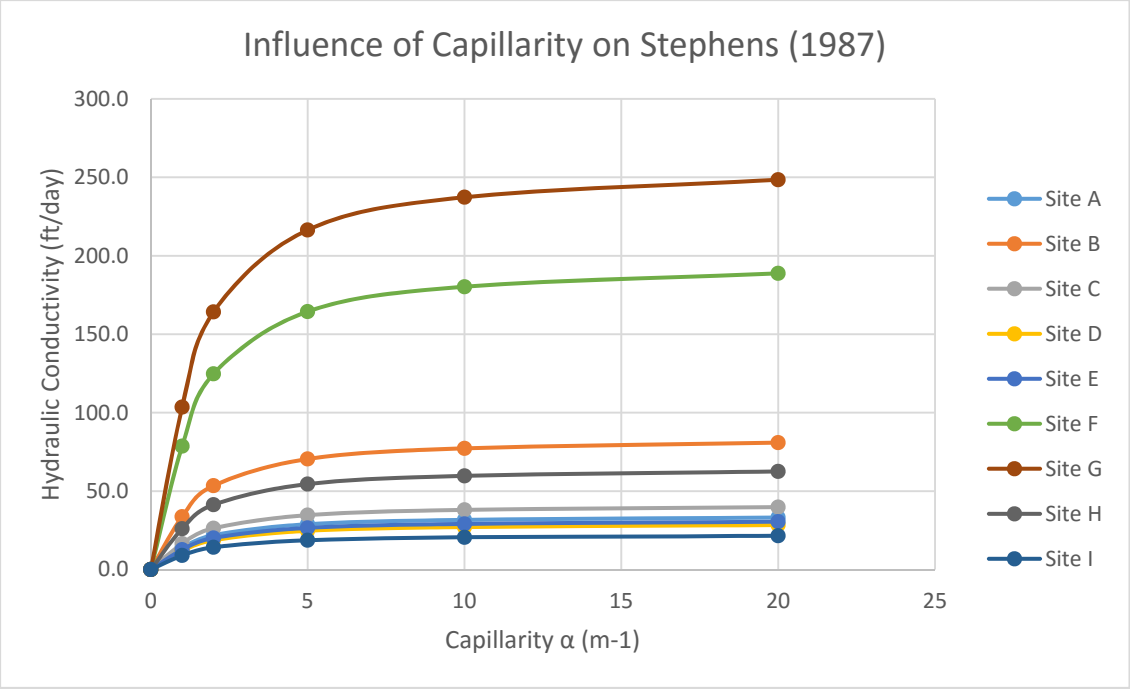

Figure 6. (b) K(α) for the Stephens (1987) solution

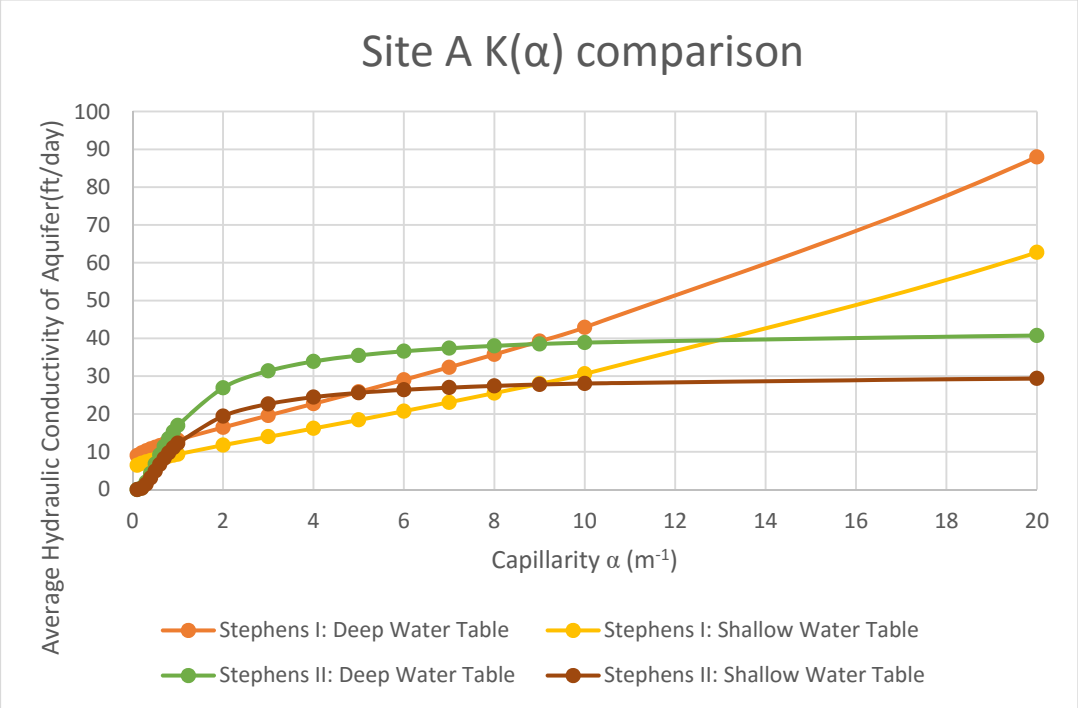

Figure 7. (a) Influence of water table depth zone for Stephens solutions

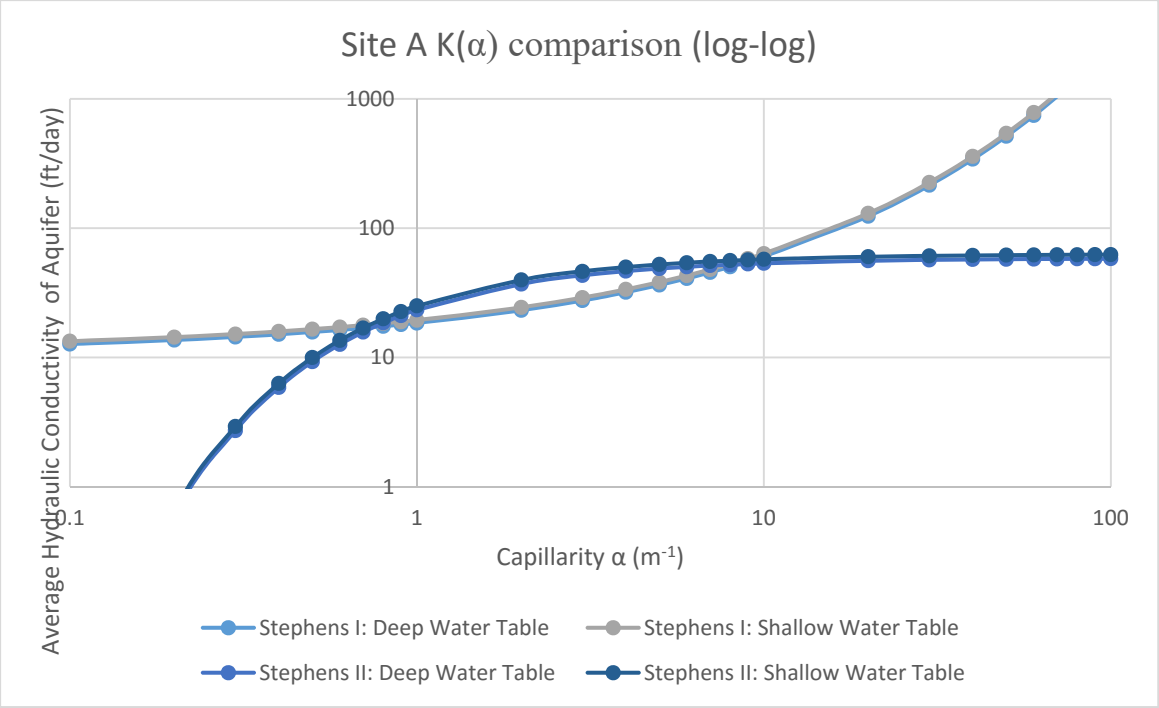

Figure 7. (b) Log-log plot of influence of water table depth zone for Stephens solutions

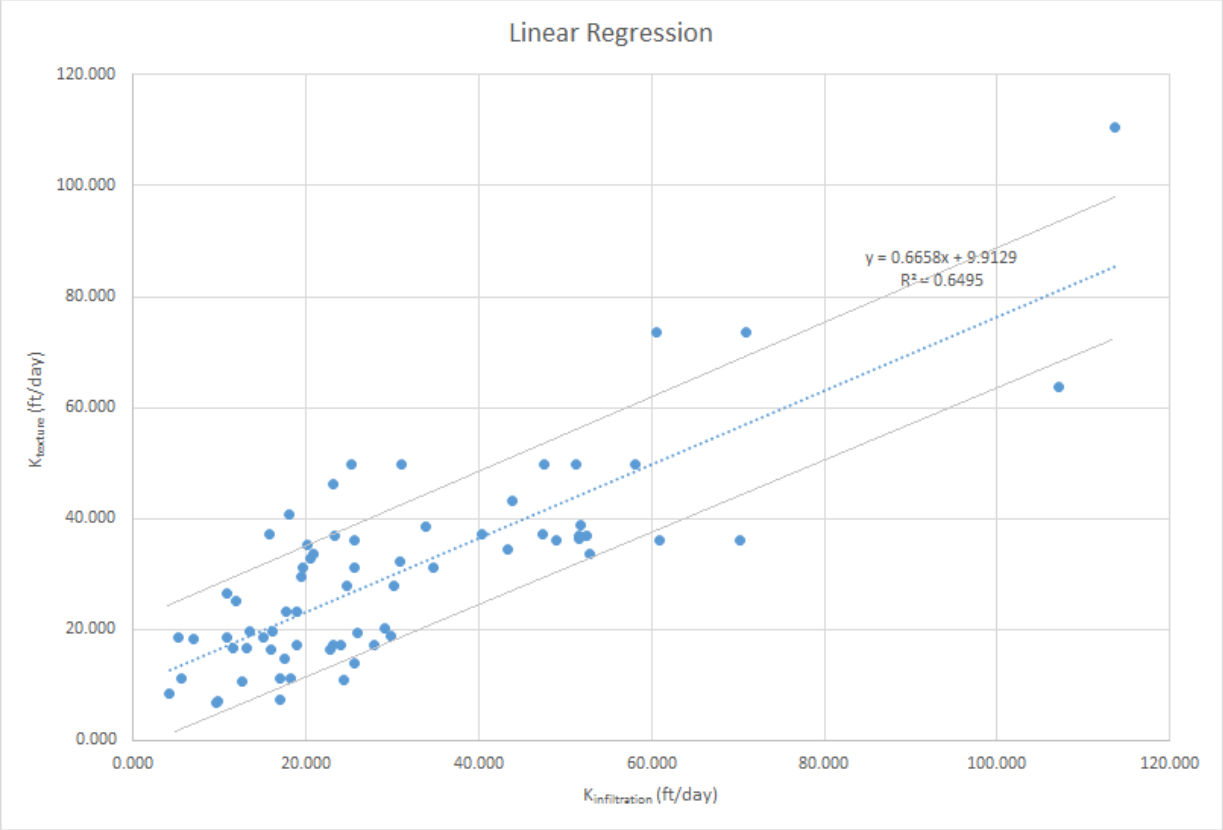

Figure 8. K from grain-size vs. K from infiltration tests with 1σ confidence interval

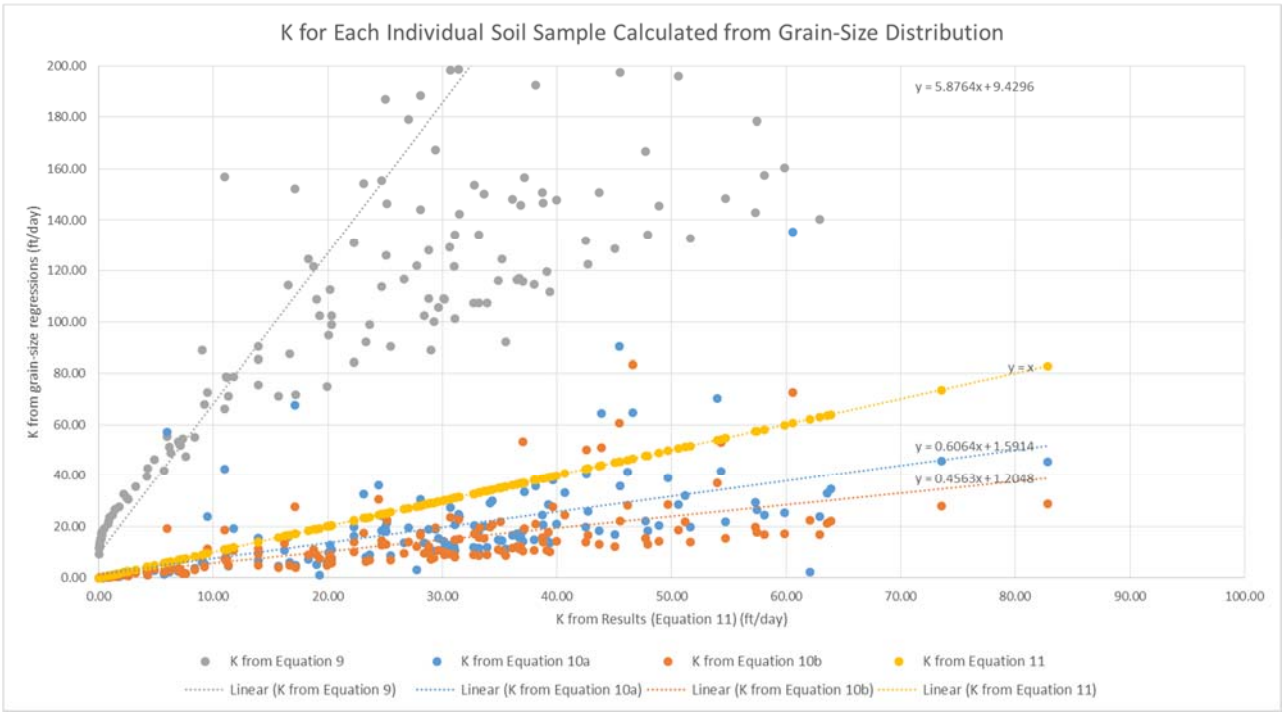

Figure 9. (a) Comparison of results with other $K(D_x)$ formulas

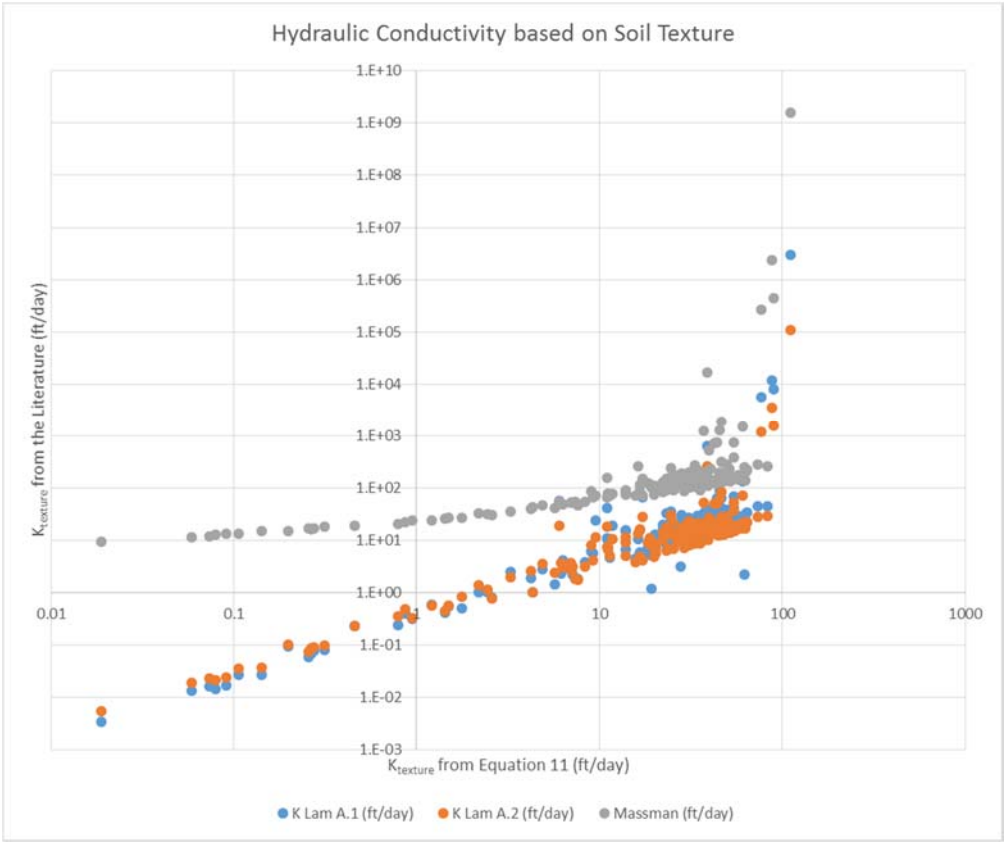

Figure 9. (b) Comparison of results with other $K(D_x)$ formulas shown on log-log plot

TABLES

Soil Type	Catalog Number	α_v, cm^{-1}
Silt "Columbia"	2001	0.015511
Silt Mont Cenis (limon Silteaux)	2002	0.013647
Silt of Nave-Yaar	2003	0.072010
Rideau clay loam	3101	0.069118
Yolo light clay	3102	0.027000
Caribou silt loam	3301	0.047125
Grenville silt loam	3302	0.030702
Ida silt loam (>15 cm)	3305	0.040000
Ida silt loam (0–15 cm)	3306	0.089975
Touched silt loam	3308	0.027302
Silt Loam G.E. 3	3310	0.004233
Gilat loam	3402	0.017000
Guelph loam	3407	0.073566
Rubicon sandy loam	3501	0.052321
Loamy Sand-Hamra Sharon	4004	0.018695
Plainfield sand (210–250 μ)	4101	0.045177
Plainfield sand (177–210 μ)	4102	0.038611
Plainfield sand (149–177 μ)	4103	0.032170
Plainfield sand (125–149 μ)	4104	0.024903
Plainfield sand (104–125 μ)	4105	0.022127
Sand	4106	0.094490
Sand	4107	0.060000
Del Norte fine sand	4108	0.016254
Oakley sand	4112	0.095194
G.E. 3 sand	4115	0.035965
Crab Creek sand	4117	0.118896
Sinai sand	4122	0.023803
Sand (50–500 μ)	4124	0.019116
Gravelly sand G.E. 9	4135	0.015048
Fine sand G.E. 2	4136	0.007192
Plainfield sand (0–25 cm)	4146	0.033730
Plainfield sand (25–60 cm)	4147	0.031813
Aggregated glass bead	5003	0.039748
Monodispersed glass bead	5004	0.036049

Table 1. Mualem's catalog of unsaturated flow parameters, adopted from Stephens et al. (1987)

Texture–structure category	Capillarity category	Sorptive number, α^* (m^{-1})
Compacted, structureless, clayey or silty materials such as landfill caps and liners, lacustrine or marine sediments, etc.	Very strong	1[b] ($0 < \alpha^* \leq 2.5$)
Porous materials that are both fine textured and massive; includes unstructured clayey and silty soils, as well as very fine to fine structureless sandy materials.	Strong	4 ($2.5 < \alpha^* \leq 8$)
Most structured and medium textured materials; includes structured clayey and loamy soils, as well as medium single-grain sands. This category is generally the most appropriate for agricultural soils.	Moderate	12 ($8 < \alpha^* \leq 24$)
Coarse and gravelly single-grain sands; may also include some highly structured soils with large and/or numerous cracks and biopores.	Weak	36 ($24 < \alpha^* \leq 68$)
Gravels, very coarse sands, etc. containing negligible amounts of coarse/medium/fine/very fine sand, silt and clay.	Negligible	100 ($68 < \alpha^* \leq \infty$)

Table 2. Representative values of the capillarity parameter, adapted from Reynolds (2013)

	Average $K_{pumping}$ (ft/day)	Average $K_{infiltration}$ (ft/day)
Site A	16.5	23
Site D	23	23.4
Site H	25	41.3

Table 3. Comparison of infiltration test results with pumping test results

Appendix A. Spreadsheet of constant-head borehole infiltration test data

well test ID	borehole Depth [D] (ft)	Length of screen open to aquifer [A] (ft)	borehole Radius [r] (ft)	Head [H] (ft)	Flow rate [Q] (gpm)	surface Elevation [z_s] (ft)	water table Elevation [z_{wt}] (ft)	Depth to water table [U] (ft)	unsaturated stratum [T_u] (ft)	% of unsaturated stratum [X]	T_u/A	WT Zone
Site A UIC 1-31; 1	66.1	25.5	0.50	27.0	32.8	489	260	229	190	14.2	7.4	1
Site A UIC 1-31; 2	66.1	25.5	0.50	62.0	103.2	489	260	229	225	27.6	8.8	1
Site A UIC 2-31	93.0	24.0	0.50	24.0	19.1	473	260	213	144	16.7	6.0	1
Site A UIC 4-32; 1	68.2	25.5	0.50	27.0	26.4	423	260	163	122	22.2	4.8	1
Site A UIC 4-32; 2	68.2	25.5	0.50	64.0	100.1	423	260	163	159	40.3	6.2	1
Site A UIC 4-32 B	68.2	25.5	0.50	51.0	27.0	423	260	163	146	35.0	5.7	1
Site A UIC 5-31; 1	100.0	14.0	0.50	14.0	28.1	373	260	113	27	51.9	1.9	2
Site A UIC 5-31; 2	100.0	27.0	0.50	27.0	95.8	373	260	113	40	67.5	1.5	2
Site A UIC 6-31; 1	90.2	15.0	0.50	15.0	19.2	361	260	101	26	58.2	1.7	2
Site A UIC 6-31; 2	90.2	32.0	0.50	32.0	103.0	361	260	101	43	74.8	1.3	2
Site A UIC 7-31; 1	62.5	9.0	0.50	9.0	23.7	462	260	202	149	6.1	16.5	1
Site A UIC 7-31; 2	62.5	23.0	0.50	23.0	104.9	462	260	202	163	14.2	7.1	1
Site A UIC 8-31	63.1	6.5	0.50	6.5	20.3	447	260	187	130	5.0	20.1	1
Site A UIC 10-31	67.1	23.0	0.50	23.0	41.0	454	260	194	150	15.3	6.5	1
Site A UIC 11-31; 1	61.1	15.0	0.50	15.0	24.3	439	260	179	133	11.3	8.9	1
Site A UIC 11-31; 2	61.1	25.0	0.50	51.0	105.2	439	260	179	169	30.2	6.8	1
Site A UIC 12-31; 1	67.9	16.0	0.50	16.0	34.5	419	260	159	107	14.9	6.7	1
Site A UIC 12-31; 2	67.9	25.0	0.50	38.0	105.7	419	260	159	129	29.4	5.2	1
Site A UIC 13-31; 1	92.9	17.0	0.50	17.0	29.8	390	260	130	54	31.4	3.2	1
Site A UIC 13-31; 2	92.9	34.0	0.50	34.0	103.2	390	260	130	71	47.8	2.1	2
Site A UIC 14-31	63.9	23.0	0.50	23.0	22.0	370	260	110	69	33.3	3.0	1
Site A UIC 15-31	64.2	21.0	0.50	21.0	25.3	333	260	73	30	70.4	1.4	2
Site A UIC 16-31; 1	74.9	15.0	0.50	15.0	28.6	451	260	191	131	11.4	8.7	1
Site A UIC 16-31; 2	74.9	25.0	0.50	25.0	98.3	451	260	191	141	17.7	5.6	1
Site A UIC 18-31; 1	67.9	15.0	0.50	15.0	41.9	432	260	172	119	12.6	7.9	1
Site A UIC 18-31; 2	67.9	24.0	0.50	24.0	104.4	432	260	172	128	18.7	5.3	1
Site A IB-1; 1	56.0	20.0	0.50	29.0	50.2	441	260	181	154	18.8	7.7	1
Site A IB-1; 2	56.0	20.0	0.50	36.0	82.0	441	260	181	161	22.4	8.1	1
Site A IB-1; 3	56.0	20.0	0.50	42.0	94.8	441	260	181	167	25.1	8.4	1
Site A IB-2	60.0	20.0	0.50	56.0	50.9	372	260	112	108	51.9	5.4	2
Site A IB-3	77.0	20.0	0.50	73.0	28.7	341	260	81	77	94.8	3.9	2
Site B UIC N-1; 1	126.2	44.2	0.25	56.0	49.2	458	315	143	73	77.0	1.6	2
Site B UIC N-1; 2	126.2	44.2	0.25	77.0	199.8	458	315	143	94	82.2	2.1	2
Site B UIC N-1; 3	126.2	44.2	0.25	87.0	276.8	458	315	143	104	83.9	2.3	2
Site B UIC N-2	126.0	44.5	0.25	84.0	268.0	458.90	315	144	102	82.4	2.3	2
Site B UIC N-3; 1	126.0	44.0	0.25	78.0	201.7	458.50	315	144	96	81.7	2.2	2
Site B UIC N-3; 2	126.0	44.0	0.25	116.0	296.4	458.50	315	144	134	86.9	3.0	2
Site B UIC S-1; 1	126.1	41.0	0.25	41.0	50.9	462	315	147	62	66.2	1.5	2
Site B UIC S-1; 2	126.1	43.1	0.25	62.0	198.7	462	315	147	83	74.8	1.9	2
Site B UIC S-1; 3	126.1	43.1	0.25	86.0	313.5	462	315	147	107	80.4	2.5	2
Site B UIC S-2; 1	125.5	40.0	0.25	40.0	51.4	462.00	315	147	62	65.0	1.5	2
Site B UIC S-2; 2	125.5	44.0	0.25	56.0	199.3	462.00	315	147	78	72.3	1.8	2
Site B UIC S-2; 3	125.5	44.0	0.25	74.0	304.7	462.00	315	147	96	77.5	2.2	2
Site B UIC S-3; 1	125.7	15.0	0.25	15.0	51.3	462.00	315	147	36	41.3	2.4	2
Site B UIC S-3; 2	125.7	30.0	0.25	30.0	204.2	462.00	315	147	51	58.5	1.7	2
Site B UIC S-3; 3	125.7	42.0	0.25	42.0	302.8	462.00	315	147	63	66.4	1.5	2
Site B UIC S-4; 1	125.5	43.8	0.25	51.0	49.4	463.45	315	148	74	69.0	1.7	2
Site B UIC S-4; 2	125.5	43.8	0.25	65.0	200.8	463.45	315	148	88	73.9	2.0	2
Site B UIC S-4; 3	125.5	43.8	0.25	88.0	310.0	463.45	315	148	111	79.3	2.5	2
Site B UIC S-5; 1	125.0	37.0	0.25	37.0	50.6	463.45	315	148	60	61.2	1.6	2
Site B UIC S-5; 2	125.0	44.0	0.25	50.0	200.3	463.45	315	148	73	68.1	1.7	2
Site B UIC S-5; 3	125.0	44.0	0.25	69.0	274.6	463.45	315	148	92	74.6	2.1	2
Site B UIC S-6; 1	125.3	25.0	0.25	25.0	49.8	463.45	315	148	48	51.9	1.9	2
Site B UIC S-6; 2	125.3	43.8	0.25	49.0	200.9	463.45	315	148	72	67.9	1.6	2
Site B UIC S-6; 3	125.3	43.8	0.25	75.0	328.4	463.45	315	148	98	76.4	2.2	2
Site B UIC S-7; 1	125.3	40.0	0.25	40.0	53.0	462.00	315	147	62	64.8	1.5	2
Site B UIC S-7; 2	125.3	43.8	0.25	53.0	200.2	462.00	315	147	75	71.0	1.7	2
Site B UIC S-7; 3	125.3	43.8	0.25	68.0	311.5	462.00	315	147	90	75.8	2.0	2
Site B UIC S-8; 1	125.6	40.0	0.25	40.0	50.2	461.25	315	146	61	66.0	1.5	2
Site B UIC S-8; 2	125.6	44.1	0.25	66.0	203.1	461.25	315	146	87	76.2	2.0	2
Site B UIC S-8; 3	125.6	44.1	0.25	96.0	313.0	461.25	315	146	117	82.3	2.6	2
Site B UIC S-10; 1	126.3	36.0	0.25	36.0	49.3	462.90	315	148	58	62.5	1.6	2
Site B UIC S-11; 1	125.8	35.0	0.25	35.0	50.4	463	315	148	57	61.2	1.6	2
Site B UIC S-11; 2	125.8	43.5	0.25	55.0	200.0	463	315	148	77	71.2	1.8	2
Site B UIC S-11; 3	125.8	43.5	0.25	65.0	290.4	463	315	148	87	74.5	2.0	2
Site B UIC S-12; 1	125.4	43.9	0.25	48.0	52.4	463.00	315	148	71	68.0	1.6	2
Site B UIC S-12; 2	125.4	43.9	0.25	83.0	201.7	463.00	315	148	106	78.6	2.4	2
Site B UIC S-12; 3	125.4	43.9	0.25	96.0	298.8	463.00	315	148	119	80.9	2.7	2
Site B UIC W-1; 1	125.4	40.0	0.25	40.0	51.1	458	315	143	58	69.3	1.4	2
Site B UIC W-1; 2	125.4	45.5	0.25	47.0	74.4	458	315	143	65	72.6	1.4	2
Site B UIC W-1; 3	125.4	45.5	0.25	56.0	148.7	458	315	143	74	75.9	1.6	2
Site B UIC W-1; 4	125.4	45.5	0.25	60.0	201.2	458	315	143	78	77.2	1.7	2
Site B UIC W-1; 5	125.4	45.5	0.25	72.0	230.9	458	315	143	90	80.2	2.0	2
Site B UIC W-2; 1	125.2	25.0	0.25	25.0	50.0	458.75	315	144	44	57.4	1.7	2
Site B UIC W-2; 2	125.2	32.0	0.25	32.0	100.1	458.75	315	144	51	63.3	1.6	2
Site B UIC W-2; 3	125.2	38.0	0.25	38.0	153.7	458.75	315	144	57	67.2	1.5	2
Site B UIC W-2; 4	125.2	44.0	0.25	44.0	199.6	458.75	315	144	63	70.3	1.4	2
Site B UIC W-2; 5	125.2	44.9	0.25	54.0	265.4	458.75	315	144	73	74.4	1.6	2
Site B UIC W-3; 1	125.4	23.0	0.25	23.0	49.6	459.00	315	144	42	55.3	1.8	2
Site B UIC W-3; 2	125.4	35.0	0.25	35.0	100.6	459.00	315	144	54	65.3	1.5	2
Site B UIC W-3; 3	125.4	41.2	0.25	56.0	274.0	459.00	315	144	75	75.1	1.8	2
Site B UIC W-4; 1	125.5	33.0	0.25	33.0	50.7	459.00	315	144	52	64.1	1.6	2
Site B UIC W-4; 2	125.5	43.0	0.25	43.0	196.2	459.00	315	144	62	69.9	1.4	2
Site B UIC W-4; 3	125.5	44.0	0.25	63.0	322.3	459.00	315	144	82	77.3	1.9	2
Site B UIC W-5; 1	125.6	43.0	0.25	43.0	49.8	459	315	144	61	70.0	1.4	2
Site B UIC W-5; 2	125.6	43.5	0.25	57.0	200.9	459	315	144	75	75.6	1.7	2
Site B UIC W-5; 3	125.6	43.5	0.25	72.0	326.1	459	315	144	90	79.6	2.1	2
Site B UIC W-6	125.5	40.0	0.25	40.0	275.8	459	315	144	59	68.4	1.5	2
Site B UIC W-7; 1	125.7	27.0	0.25	27.0	52.8	460.50	315	146	47	57.7	1.7	2
Site B UIC W-7; 2	125.7	44.4	0.25	50.0	197.4	460.50	315	146	70	71.6	1.6	2
Site B UIC W-7; 3	125.7	44.4	0.25	62.0	282.7	460.50	315	146	82	75.8	1.8	2
Site B UIC W-8; 1	125.8	34.0	0.25	34.0	47.7	460.50	315	146	54	63.3	1.6	2
Site B UIC W-8; 2	125.8	43.8	0.25	48.0	196.1	460.50	315	146	68	70.9	1.5	2
Site B UIC W-8; 3	125.8	43.8	0.25	64.0	305.1	460.50	315	146	84	76.5	1.9	2
Site B UIC W-9; 1	125.5	25.0	0.25	25.0	49.8	460.50	315	146	45	55.6	1.8	2
Site B UIC W-9; 2	125.5	34.0	0.25	34.0	202.1	460.50	315	146	54	63.0	1.6	2
Site B UIC W-9; 3	125.5	44.0	0.25	53.0	308.3	460.50	315	146	73	72.6	1.7	2
Site B UIC W-10; 1	125.3	26.0	0.25	26.0	50.5	460.50	315	146	46	56.3	1.8	2
Site B UIC W-10; 2	125.3	44.3	0.25	51.0	204.0	460.50	315	146	71	71.6	1.6	2
Site C UIC 2; 1	81.5	25.0	0.92	25.0	50.0	360	225	135	79	31.8	3.1	1
Site C UIC 2; 2	81.5	37.5	0.92	37.5	100.0	360	225	135	91	41.2	2.4	2
Site C UIC 4; 1	81.5	30.0	0.92	30.0	50.0	360	225	135	84	35.9	2.8	2
Site C UIC 4; 2	81.5	40.0	0.92	40.0	75.0	360	225	135	94	42.8	2.3	2
Site C UIC 5; 1	83.5	24.0	0.92	24.0	50.0	360	225	135	76	31.8	3.1	1
Site C UIC 5; 2	83.5	34.0	0.92	34.0	100.0	360	225	135	86	39.8	2.5	2
Site C UIC 6; 1	82.0	29.0	0.92	29.0	50.0	350	225	125	72	40.3	2.5	2
Site C UIC 6; 2	82.0	32.0	0.92	32.0	60.0	350	225	125	75	42.7	2.3	2
Site C UIC 7; 1	83.5	17.5	0.92	17.5	50.0	350	225	125	59	29.7	3.4	1
Site C UIC 7; 2	83.5	27.0	0.92	27.0	100.0	350	225	125	69	39.4	2.5	2
Site C UIC 8; 1	80.0	17.0	0.92	17.0	50.0	340	225	115	52	32.7	3.1	1
Site C UIC 8; 2	80.0	32.0	0.92	32.0	100.0	340	225	115	67	47.8	2.1	2
Site D UIC 1; 1	75.0	30.0	0.25	50.0	84.6	390	308	82	57	87.7	1.9	2
Site D UIC 1; 2	75.0	30.0	0.25	76.0	124.2	390	308	82	83	91.6	2.8	2
Site D UIC 2; 1	80.5	30.0	0.25	34.0	9.9	402	308	94	48	71.6	1.6	2
Site D UIC 2; 2	80.5	30.0	0.25	70.0	81.0	402	308	94	84	83.8	2.8	2
Site D UIC 2; 3	80.5	30.0	0.25	81.0	104.5	402	308	94	95	85.7	3.2	2
Site E DD-1; 1	35.1	2.5	1.25	2.5	5.2	334	292	42	9	26.6	3.8	1
Site E DD-1; 2	35.1	4.5	1.25	4.5	9.3	334	292	42	11	39.5	2.5	2
Site E DD-1; 3	35.1	9.0	1.25	9.0	20.8	334	292	42	16	56.6	1.8	2
Site E DD-1; 4	35.1	16.0	1.25	16.0	40.5	334	292	42	23	69.9	1.4	2
Site E DD-1; 5	35.1	21.0	1.25	21.0	55.0	334	292	42	28	75.3	1.3	2
Site E DD-2	40.0	28.0	1.25	28.0	50.6	380	292	88	76	36.8	2.7	2
Site F UIC 1	130.0	40.0	0.42	38.0	226.0	283	79	204	112	33.9	2.8	1
Site F UIC 2	138.0	40.0	0.42	28.0	267.0	282	79	203	93	30.1	2.3	1
Site I UIC 1; 1	31.5	10.0	0.25	22.5	10.0	103	25	78	69	32.6	6.9	1
Site I UIC 1; 2	31.5	10.0	0.25	27.5	15.0	103	25	78	74	37.2	7.4	1
Site I UIC 2; 1	40.3	10.0	0.25	17.0	15.0	110	25	85	62	27.5	6.2	1
Site I UIC 2; 2	40.3	10.0	0.25	20.0	20.0	110	25	85	65	30.9	6.5	1
Site I UIC 2; 3	40.3	10.0	0.25	24.0	25.0	110	25	85	69	34.9	6.9	1
Site G	80.0	9.0	2.17	9.0	143.0			130	59	15.3	6.6	1
Site H PD-7	153.5	1.3	0.67	1.3	24.0	875	625	250	98	1.3	75.2	1
Site H PD-56	90.0	20.0	0.83	33.0	41.0	800	625	175	118	28.0	5.9	1
Site H PD-59	90.0	12.0	0.83	12.0	51.0	800	625	175	97	12.4	8.1	1
Site H PD-62	90.0	13.5	0.83	13.5	46.0	800	625	175	99	13.7	7.3	1

Appendix B. Spreadsheet of constant-head borehole infiltration test results

	Method:		*Stephens (1979) with α =*							
Location	*Glover*	*Stephens' sand 4107*	0	1	2	5	10	20	100	∞
Site A	5.9	23.2	6.1	10.6	13.3	20.9	34.7	71.2	1472.9	∞
Site B	10.1	66.4	15.7	27.2	34.1	53.5	88.8	182.1	3766.0	∞
Site C	6.5	25.9	7.5	12.9	16.2	25.4	42.2	86.5	1789.4	∞
Site D	4.0	23.4	5.5	9.5	12.0	18.8	31.2	63.9	1322.5	∞
Site E	5.9	20.1	6.3	10.9	13.7	21.5	35.8	73.4	1517.2	∞
Site F	28.6	133.1	34.6	59.8	75.0	117.7	195.5	400.7	8288.8	∞
Site G	61.1	168.3	60.2	104.1	130.6	204.9	340.4	697.8	14432.8	∞
Site H	12.5	41.3	12.1	20.9	26.2	41.2	68.4	140.2	2899.5	∞
Site I	5.0	15.9	4.0	7.0	8.8	13.8	22.9	46.9	969.9	∞
	Method:		Stephens (1987) with α =							
Location	*Glover*	*Stephens' sand 4107*	0	1	2	5	10	20	100	∞
Site A	5.9	23.2	0.0	13.8	21.9	28.9	31.7	33.2	34.4	34.7
Site B	10.1	66.4	0.0	33.7	53.5	70.5	77.3	80.9	83.9	84.7
Site C	6.5	25.9	0.0	16.6	26.3	34.7	38.0	39.8	41.3	41.7
Site D	4.0	23.4	0.0	11.8	18.7	24.7	27.1	28.4	29.4	29.7
Site E	5.9	20.1	0.0	12.7	20.2	26.6	29.1	30.5	31.7	31.9
Site F	28.6	133.1	0.0	78.7	124.7	164.4	180.3	188.8	195.9	197.7
Site G	61.1	168.3	0.0	103.6	164.2	216.4	237.3	248.5	257.8	260.2
Site H	12.5	41.3	0.0	26.1	41.3	54.5	59.7	62.6	64.9	65.5
Site I	5.0	15.9	0.0	9.0	14.2	18.8	20.6	21.5	22.3	22.5

Appendix C. Particle-size distribution of soil samples by location

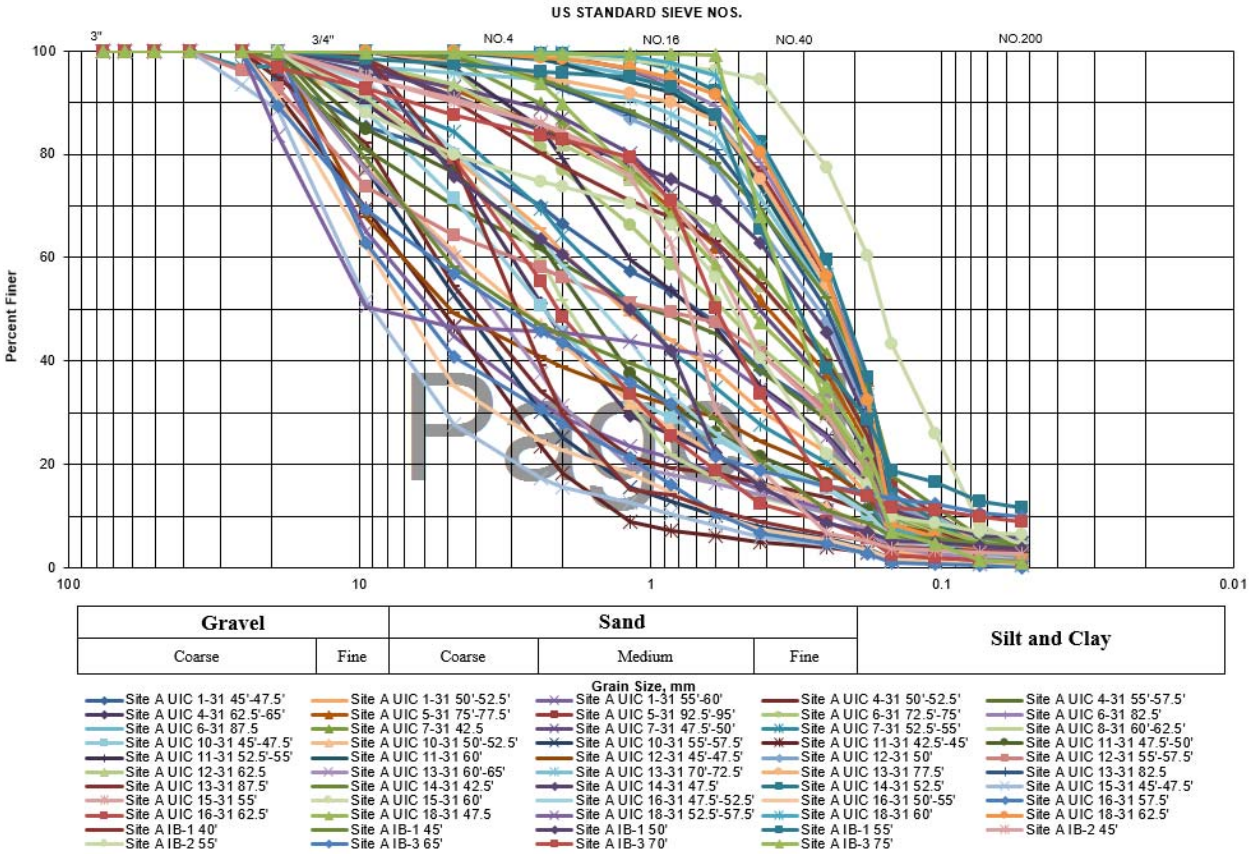

(a) Grain-size curves for Site A

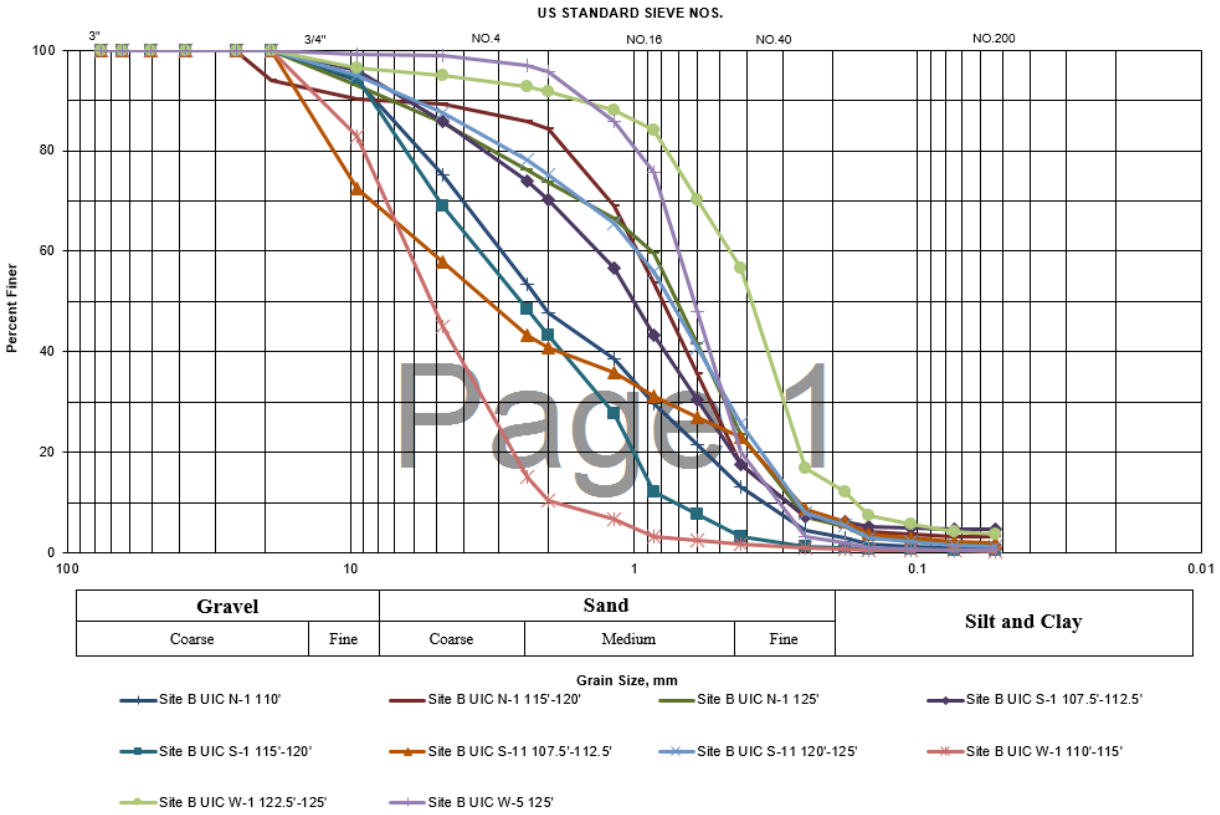

(b) Grain-size curves for Site B

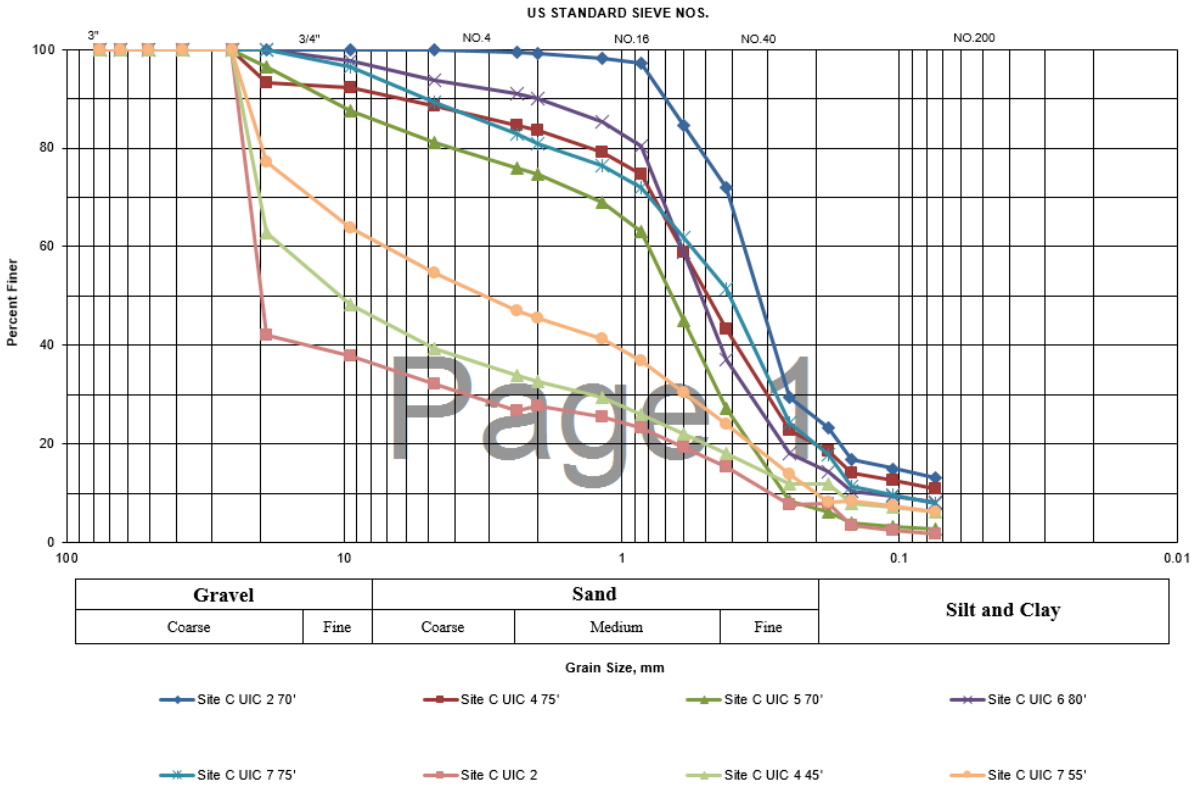

(c) Grain-size curves for Site C

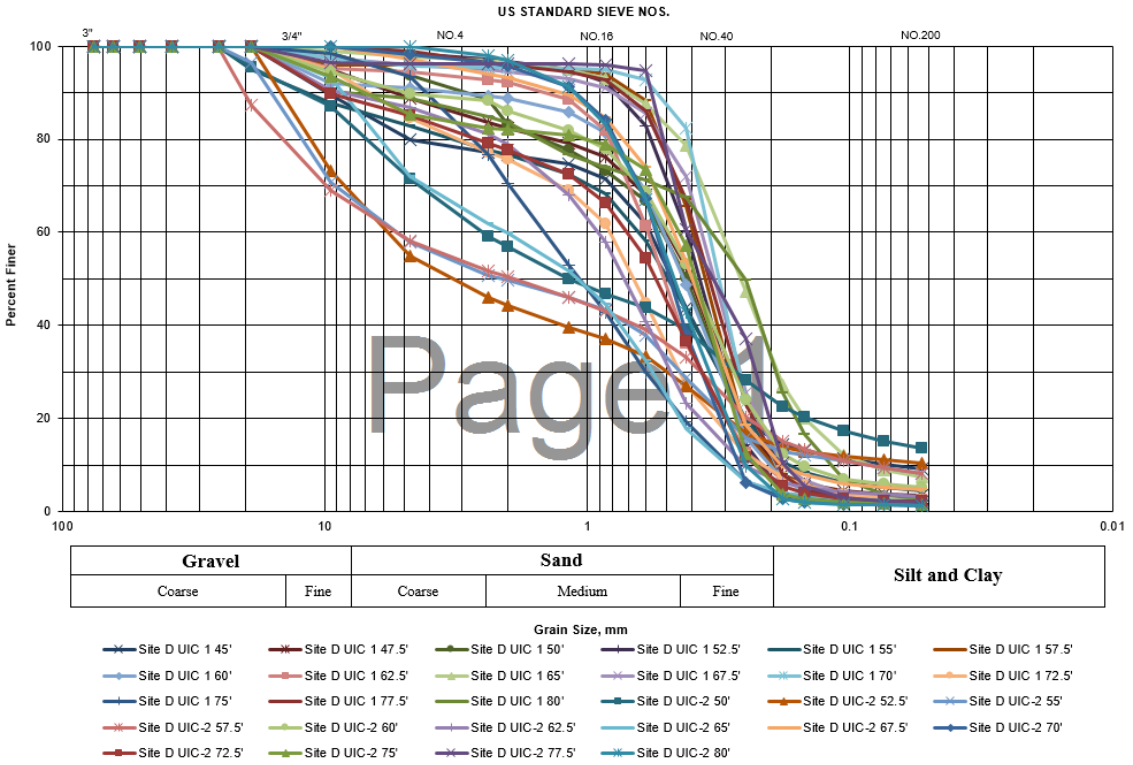

(d) Grain-size curves for Site D

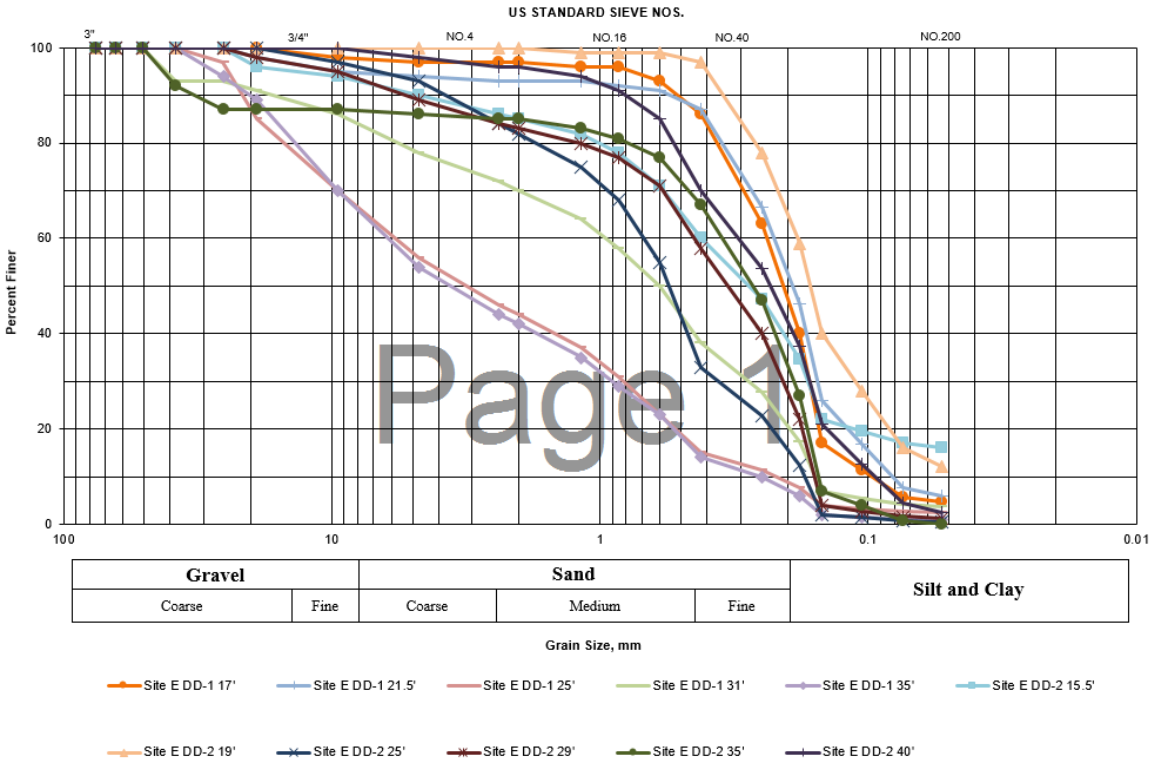

(e) Grain-size curves for Site E

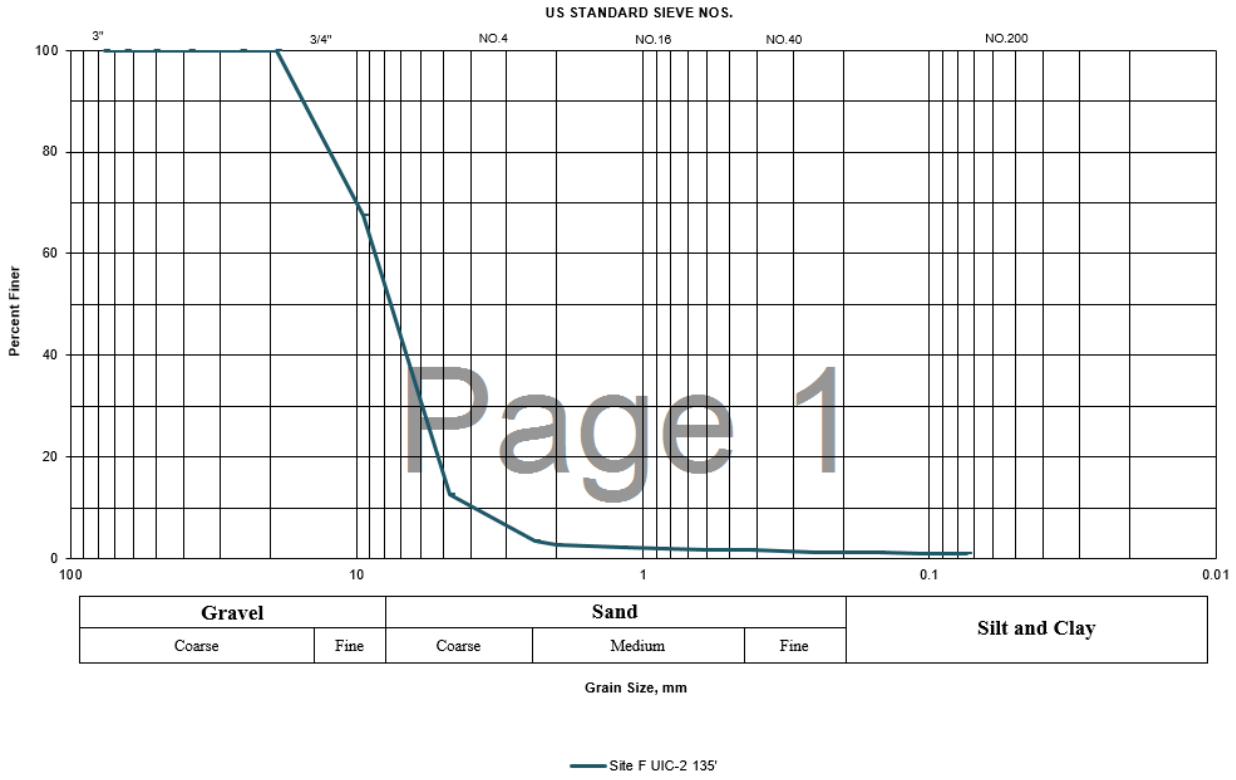

(f) Grain-size curves for Site F

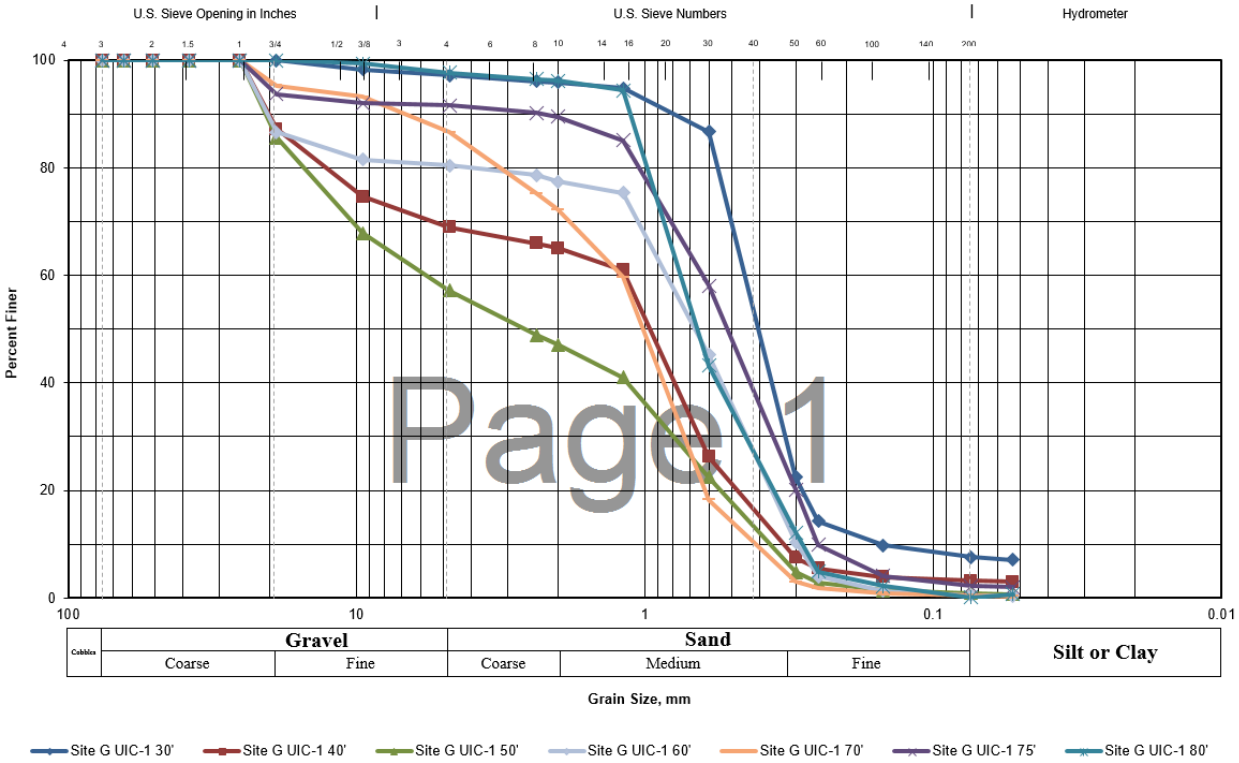

(g) Grain-size curves for Site G

Appendix D

Well ID	Sample Depth (ft)	D_{10} (mm)	D_{60} (mm)	D_{90} (mm)	f_{fines}	$logK_{GS}$
Site A UIC 1-31	45'-47.5'	0.116	1.410	14.340	0.056	1.040
	50'-52.5'	0.203	1.931	9.548	0.035	1.399
	55'-60'	0.299	8.051	16.308	0.019	1.547
Site A UIC 4-31	50'-52.5'	0.216	5.496	12.312	0.058	1.264
	55'-57.5'	0.152	2.143	14.118	0.060	1.048
	62.5'-65'	0.310	2.926	9.729	0.014	1.610
Site A UIC 5-31	55'-57.5'	0.136	0.326	1.058	0.048	1.515
	75'-77.5'	0.152	0.556	3.493	0.033	1.562
	92.5'-95'	0.124	0.311	0.721	0.052	1.493
Site A UIC 6-31	40'-42.5'	0.153	1.748	5.532	0.043	1.460
	50'-52.5'	0.120	0.397	1.196	0.066	1.368
	72.5'-75'	0.153	0.900	3.289	0.038	1.543
	82.5'	0.133	0.322	0.628	0.049	1.521
	87.5'	0.156	0.341	0.691	0.025	1.713
Site A UIC 7-31	42.5'	0.151	0.465	2.373	0.037	1.564
	47.5'-50'	0.170	0.555	2.767	0.028	1.628
	52.5'-55'	0.202	1.704	8.168	0.028	1.493
Site A UIC 8-31	40'	0.146	0.387	1.216	0.041	1.568
	47.5'-50'	0.181	1.439	9.329	0.034	1.393
	52.5'-55'	0.701	5.211	12.119	0.014	1.658
	60'-62.5'	0.315	2.381	8.947	0.024	1.536
Site A UIC 10-31	40'-42.5'	0.198	3.036	9.789	0.024	1.521
	45'-47.5'	0.231	3.157	10.192	0.024	1.516
	50'-52.5'	0.301	4.542	14.920	0.015	1.488
	55'-57.5'	0.581	5.807	14.291	0.008	1.643
Site A UIC 11-31	42.5'-45'	1.321	6.951	18.223	0.013	1.590
	47.5'-50'	0.223	2.200	11.670	0.034	1.348
	52.5'-55'	0.201	1.198	2.850	0.039	1.566
	60'	0.149	0.353	0.712	0.040	1.593
Site A UIC 12-31	45'-47.5'	0.183	7.737	15.240	0.054	1.280
	50'	0.137	0.385	1.530	0.064	1.374
	55'-57.5'	0.163	2.867	17.288	0.038	1.145
	62.5'	0.149	0.488	3.526	0.043	1.478
Site A UIC 13-31	60'-65'	0.298	4.744	14.395	0.017	1.498
	70'-72.5'	0.126	0.349	1.088	0.054	1.466
	77.5'	0.132	0.333	0.834	0.047	1.530
	82.5'	0.142	0.364	1.547	0.038	1.580
	87.5'	0.145	0.507	4.649	0.039	1.472
Site A UIC 14-31	42.5'	0.111	0.342	1.381	0.060	1.406

	47.5'	0.143	0.402	4.162	0.062	1.301
	52.5'	0.132	0.306	0.529	0.040	1.595
Site A UIC 15-31	40'-42.5'	2.018	5.992	10.662	0.004	1.952
	45'-47.5'	0.792	10.988	20.103	0.008	1.670
	55'	0.211	0.610	4.615	0.026	1.587
	60'	0.079	0.187	0.310	0.085	1.235
Site A UIC 16-31	42.5'-45'	2.408	12.284	18.650	0.007	1.943
	47.5'-52.5'	0.221	2.104	7.447	0.029	1.527
	50'-55'	0.574	9.114	18.446	0.008	1.631
	57.5'	0.568	8.905	16.016	0.004	1.737
	62.5'	0.373	2.652	8.001	0.014	1.664
Site A UIC 18-31	47.5'	0.144	0.637	2.015	0.050	1.479
	52.5'-57.5'	0.185	13.570	21.081	0.037	1.446
	60'	0.163	0.338	0.495	0.030	1.680
	62.5'	0.157	0.329	0.550	0.033	1.654
Site A IB-1	20'	0.044	1.019	13.541	0.123	0.512
	30'	0.007	0.557	4.655	0.203	0.156
	32.5'	0.167	0.475	1.058	0.052	1.492
	40'	0.498	3.431	7.000	0.032	1.599
	45'	0.214	5.051	14.036	0.047	1.275
	50'	0.275	1.942	7.396	0.041	1.432
	55'	0.034	0.377	0.701	0.128	0.882
Site A IB-2	25'	0.001	3.706	13.225	0.214	-0.100
	35'	0.172	0.501	3.759	0.049	1.426
	45'	0.288	0.824	4.202	0.029	1.594
	55'	0.149	0.683	10.621	0.068	1.046
Site A IB-3	10'	0.000	0.334	3.078	0.371	-1.136
	25'	0.002	0.575	4.638	0.295	-0.575
	55'	0.118	3.425	10.873	0.079	1.054
	65'	0.055	5.643	19.315	0.107	0.625
	70'	0.074	0.707	6.593	0.100	0.922
	75'	0.156	0.375	0.540	0.015	1.799
Site B UIC N-1	110'	0.348	2.939	8.238	0.010	1.697
	115'-120'	0.288	0.974	7.727	0.033	1.448
	125'	0.273	0.870	7.156	0.018	1.581
Site B UIC S-1	107.5'-112.5'	0.289	1.340	6.330	0.047	1.399
	115-120'	0.718	3.513	8.421	0.006	1.783
Site B UIC S-11	107.5'-112.5'	0.262	5.262	14.786	0.021	1.469
	120'-125'	0.266	0.978	5.940	0.014	1.658
Site B UIC W-1	110'-115'	1.913	6.253	12.676	0.004	1.883
	122.5'-125'	0.166	0.458	1.552	0.043	1.546
Site B UIC W-5	125'	0.309	0.698	1.478	0.006	1.867
Site C UIC 2		0.291	20.779	24.156	0.017	1.798
	70'	0.068	0.363	0.695	0.131	0.866
Site C UIC 4	45'	0.164	16.596	23.491	0.061	1.289

	75'	0.072	0.614	6.276	0.110	0.850
Site C UIC 5	40'	0.705	15.927	25.161	0.022	1.572
	70'	0.262	0.801	11.433	0.027	1.364
Site C UIC 6	45'	0.119	0.796	8.055	0.089	0.966
	80'	0.130	0.612	1.974	0.082	1.221
Site C UIC 7	55'	0.199	7.140	22.370	0.062	0.956
	75'	0.114	0.564	5.056	0.078	1.144
Site D UIC 1	30'	0.010	0.818	10.128	0.190	0.084
	32.5'	0.014	1.073	7.754	0.190	0.175
	35'	0.005	0.326	3.094	0.383	-1.232
	37.5'	0.089	6.581	18.896	0.093	0.791
	40'	0.010	0.365	5.719	0.220	-0.023
	42.5'	0.185	0.545	5.528	0.057	1.305
	45'	0.072	0.579	9.829	0.101	0.798
	47.5'	0.193	0.499	5.393	0.038	1.459
	50'	0.201	0.518	2.896	0.031	1.602
	52.5'	0.218	0.419	0.781	0.020	1.759
	55'	0.169	0.639	11.704	0.051	1.144
	57.5'	0.195	0.396	0.667	0.035	1.640
	60'	0.201	0.513	3.040	0.032	1.589
	62.5'	0.215	0.589	1.449	0.028	1.679
	65'	0.084	0.309	0.700	0.089	1.195
	67.5'	0.181	0.368	0.794	0.028	1.689
	70'	0.191	0.345	0.546	0.018	1.777
	72.5'	0.214	0.818	6.796	0.029	1.498
	75'	0.290	1.457	4.123	0.018	1.709
	77.5'	0.188	0.386	0.733	0.019	1.764
	80'	0.118	0.338	8.281	0.038	1.347
Site D UIC-2	2.5'	0.012	0.225	0.663	0.345	-0.850
	5'	0.009	0.226	0.726	0.369	-1.043
	7.5'	0.008	0.304	3.635	0.348	-0.972
	10'	0.009	0.538	9.950	0.288	-0.701
	12.5'	0.008	0.319	2.558	0.305	-0.593
	15'	0.006	0.229	0.804	0.376	-1.102
	17.5'	0.009	0.358	3.706	0.289	-0.503
	20'	0.009	0.344	4.419	0.293	-0.560
	22.5'	0.014	3.185	15.346	0.198	-0.064
	25'	0.020	0.111	0.381	0.456	-1.727
	27.5'	0.015	0.665	10.472	0.241	-0.339
	30'	0.400	7.225	15.934	0.060	1.211
	32.5'	0.049	4.674	17.983	0.144	0.337
	35'	0.159	0.373	19.364	0.038	0.976
	37.5'	0.074	5.080	13.600	0.100	0.855
	40'	0.362	10.354	16.324	0.034	1.523
	42.5'	0.017	5.493	16.059	0.167	0.249

	45'	0.205	0.571	1.700	0.042	1.557
	47.5'	0.138	0.364	3.607	0.045	1.454
	50'	0.025	2.504	12.107	0.152	0.386
	52.5'	0.040	5.788	14.676	0.111	0.755
	55'	0.088	5.356	15.992	0.093	0.841
	57.5'	0.085	5.364	20.210	0.094	0.690
	60'	0.153	0.491	4.832	0.059	1.307
	62.5'	0.253	0.912	8.500	0.036	1.392
	65'	0.294	2.035	8.562	0.024	1.534
	67.5'	0.182	0.470	1.267	0.052	1.486
	70'	0.266	0.548	1.111	0.014	1.805
	72.5'	0.230	0.705	9.575	0.023	1.448
	75'	0.228	0.448	7.112	0.017	1.569
	77.5'	0.178	0.415	0.571	0.023	1.738
	80'	0.251	0.541	1.123	0.014	1.803
Site E DD-1	17'	0.098	0.240	0.515	0.056	1.462
	21.5'	0.081	0.224	0.549	0.076	1.300
	25'	0.222	5.801	21.443	0.026	1.220
	31'	0.157	0.948	16.544	0.041	1.070
	35'	0.250	6.171	20.136	0.011	1.401
Site E DD-2	15.5'	0.007	0.420	4.760	0.170	0.409
	19'	0.045	0.183	0.347	0.160	0.633
	25'	0.172	0.686	3.778	0.008	1.758
	29'	0.159	0.444	5.342	0.016	1.630
	35'	0.153	0.350	32.396	0.007	0.777
	40'	0.094	0.306	0.802	0.044	1.550
Site F UIC-2	135'	3.899	8.650	15.355	0.010	2.043
Site G UIC-1	30'	0.152	0.450	0.793	0.076	1.308
	40'	0.329	1.167	20.246	0.032	1.042
	50'	0.368	5.705	20.762	0.009	1.389
	60'	0.297	0.840	20.452	0.005	1.233
	70'	0.412	1.205	6.799	0.004	1.732
	75'	0.250	0.630	2.265	0.022	1.704
	80'	0.284	0.751	1.122	0.001	1.918

(a) Grain-size parameters in used in linear regression

d_{10}	d_{60}	d_{90}	F_{fines}	Constant			
0.102	0.039	-0.034	-7.952	1.906	<--	coefficients of regression formula	
Well Test ID	WT Zone	Overconsolidated?	K_{INF}	$logK_{INF}$	$logK_{GS}$	K_{GS}	$(\Delta K)^2$
Site A UIC 1-31; 1	1	Yes	13.398	1.127	1.291	19.563	38.009
Site A UIC 1-31; 2	1	Yes	16.045	1.205	1.291	19.563	12.379
Site A UIC 4-31; 1	1	Yes	10.784	1.033	1.268	18.517	59.807
Site A UIC 4-31; 2	1	Yes	14.999	1.176	1.268	18.517	12.378
Site A UIC 4-31 B	1	Yes	5.267	0.722	1.268	18.517	175.564
Site A UIC 5-31; 1	2	Yes	25.534	1.407	1.493	31.089	30.860
Site A UIC 5-31; 2	2	Yes	52.828	1.723	1.526	33.610	369.337
Site A UIC 6-31; 1	2	Yes	18.083	1.257	1.611	40.851	518.392
Site A UIC 6-31; 2	2	Yes	51.690	1.713	1.588	38.698	168.785
Site A UIC 7-31; 1	1	Yes	34.700	1.540	1.493	31.101	12.956
Site A UIC 7-31; 2	1	Yes	51.625	1.713	1.560	36.293	235.059
Site A UIC 8-31	1	Yes	43.381	1.637	1.536	34.368	81.239
Site A UIC 10-31	1	Yes	20.177	1.305	1.546	35.164	224.584
Site A UIC 11-31; 1	1	Yes	19.652	1.293	1.494	31.163	132.511
Site A UIC 11-31; 2	1	Yes	20.523	1.312	1.517	32.853	152.032
Site A UIC 12-31; 1	1	Yes	25.885	1.413	1.290	19.512	40.613
Site A UIC 12-31; 2	1	Yes	29.025	1.463	1.308	20.308	76.000
Site A UIC 13-31; 1	1	Yes	20.838	1.319	1.526	33.586	162.521
Site A UIC 13-31; 2	2	Yes	30.843	1.489	1.508	32.211	1.873
Site A UIC 14	1	Yes	10.827	1.035	1.424	26.567	247.734
Site A UIC 15	2	Yes	19.472	1.289	1.472	29.629	103.162
Site A UIC 16; 1	1	Yes	23.129	1.364	1.664	46.177	531.187
Site A UIC 16; 2	1	Yes	43.909	1.643	1.636	43.273	0.405
Site A UIC 18; 1	1	Yes	33.885	1.530	1.586	38.558	21.836
Site A UIC 18; 2	1	Yes	48.900	1.689	1.558	36.142	162.767
Site A IB-1; 1	1	Yes	18.872	1.276	1.234	17.140	2.997
Site A IB-1; 2	1	Yes	23.977	1.380	1.234	17.140	46.744
Site A IB-1; 3	1	Yes	23.174	1.365	1.234	17.140	36.406
Site A IB-2	2	Yes	6.928	0.841	1.263	18.320	129.773
Site A IB-3	2	Yes	4.145	0.618	0.926	8.428	18.348
Site B UIC N-1; 1	2	Yes	15.664	1.195	1.569	37.050	457.336
Site B UIC N-1; 2	2	Yes	40.356	1.606	1.569	37.050	10.929
Site B UIC N-1; 3	2	Yes	47.330	1.675	1.569	37.050	105.686
Site B UIC S-1; 1	2	Yes	23.268	1.367	1.568	36.946	187.064
Site B UIC S-1; 2	2	Yes	51.653	1.713	1.568	36.946	216.303
Site B UIC S-1; 3	2	Yes	52.523	1.720	1.568	36.946	242.652
Site B UIC S-11; 1	2	Yes	25.580	1.408	1.558	36.124	111.171
Site B UIC S-11; 2	2	Yes	60.839	1.784	1.558	36.124	610.804
Site B UIC S-11; 3	2	Yes	70.160	1.846	1.558	36.124	1158.408
Site B UIC W-1; 1	2	Yes	25.139	1.400	1.698	49.875	611.892
Site B UIC W-1; 2	2	Yes	31.083	1.493	1.698	49.875	353.164
Site B UIC W-1; 3	2	Yes	47.484	1.677	1.698	49.875	5.719
Site B UIC W-1; 4	2	Yes	58.025	1.764	1.698	49.875	66.411
Site B UIC W-1; 5	2	Yes	51.304	1.710	1.698	49.875	2.042
Site B UIC W-5; 2	2	Yes	60.623	1.783	1.867	73.564	167.460
Site B UIC W-5; 3	2	Yes	70.842	1.850	1.867	73.564	7.406
Site C UIC 2; 1	1	Yes	16.931	1.229	0.866	7.339	91.998
Site C UIC 2; 2	2	Yes	17.422	1.241	1.169	14.742	7.184
Site C UIC 4; 1	2	Yes	9.843	0.993	0.850	7.076	7.655
Site C UIC 4; 2	2	Yes	12.585	1.100	1.024	10.577	4.033
Site C UIC 5; 1	1	Yes	17.753	1.249	1.364	23.135	28.968
Site C UIC 5; 2	2	Yes	18.840	1.275	1.364	23.135	18.452
Site C UIC 6; 1	2	Yes	11.478	1.060	1.221	16.651	26.763
Site C UIC 6; 2	2	Yes	13.014	1.114	1.221	16.651	13.234
Site C UIC 7; 1	1	Yes	25.625	1.409	1.144	13.936	136.649
Site C UIC 7; 2	2	Yes	24.410	1.388	1.041	11.001	179.800
Site D UIC 1; 1	2	Yes	30.106	1.479	1.443	27.753	5.537
Site D UIC 1; 2	2	Yes	24.652	1.392	1.443	27.753	9.618
Site D UIC 2; 1	2	Yes	5.607	0.749	1.051	11.242	31.750
Site D UIC 2; 2	2	Yes	17.019	1.231	1.051	11.242	33.371
Site D UIC 2; 3	2	Yes	18.201	1.260	1.051	11.242	48.427
Site E DD-1; 1	1	Yes	11.803	1.072	1.401	25.183	179.017
Site E DD-1; 2	2	Yes	15.825	1.199	1.214	16.351	0.276
Site E DD-1; 3	2	Yes	22.681	1.356	1.216	16.431	39.058
Site E DD-1; 4	2	Yes	27.934	1.446	1.236	17.206	115.086
Site E DD-1; 5	2	Yes	29.795	1.474	1.275	18.846	119.880
Site E DD-2	2	Yes	9.605	0.982	0.841	6.932	7.141
Site F UIC 2	1	Yes	113.635	2.056	2.043	110.493	9.869
Site G	1	Yes	107.049	2.030	1.805	63.789	1871.451
						Sum of Squares:	11105.922

(b) Least-squares fit between $K_{infiltration}$ and $K_{texture}$ using Excel Solver